

# Thermodynamic geometry of black holes in $f(R)$ gravity

Saheb Soroushfar, Reza Saffari <sup>a</sup>, Negin Kamvar

Department of Physics, University of Guilan, 41335-1914 Rasht, Iran

Received: 9 May 2016 / Accepted: 8 August 2016 / Published online: 27 August 2016  
© The Author(s) 2016. This article is published with open access at Springerlink.com

**Abstract** In this paper, we consider three types (static, static charged, and rotating charged) of black holes in  $f(R)$  gravity. We study the thermodynamical behavior, stability conditions, and phase transition of these black holes. It is shown that the number and type of phase transition points are related to different parameters, which shows the dependency of the stability conditions to these parameters. Also, we extend our study to different thermodynamic geometry methods (Ruppeiner, Weinhold, and GTD). Next, we investigate the compatibility of curvature scalar of geothermodynamic methods with phase transition points of the above black holes. In addition, we point out the effect of different values of the spacetime parameters on the stability conditions of mentioned black holes.

## 1 Introduction

The black hole is one of the most fascinating predictions of Einstein's theory of General Relativity, which has been an adsorbent subject in theoretical physics for many years, and it has unknown issues yet. One of the most interesting aspects of studying black holes is thermodynamics. The studies of black holes as a thermodynamic system have started with the famous work of Hawking and Bekenstein [1–3], which is followed by other pioneering research of Padmanabhan [4,5]. According to black hole thermodynamics, the thermodynamic quantities of a black hole such as entropy and temperature are related to its geometrical quantities such as the horizon area and surface gravity [2,6]. In recent years, the research on the thermodynamic properties of the black holes has revealed a lot of interesting aspects. One of these aspects is the stability of black holes. The heat capacity of a black hole must be positive in order for it to be in thermal stability [7–10]. Studying the heat capacity of a black hole provides a mechanism to study the phase transitions of

the black holes. There are two types of phase transition; in the first one, the changes in the sign of the heat capacity denote a type of phase transition, in other words, the roots of the heat capacity represent phase transition points, so we call these phase transitions type one. Another kind of phase transition is obtained from divergencies of the heat capacity. This kind of phase transition is called a phase transition of type two [7–10]. Some work on the normal thermodynamics of black holes shows that in many cases one cannot identify the detailed reasons for irregularities of mass, temperature, and heat capacity shown by the system. During the last few decades, many efforts have been made to introduce different concepts of geometry into ordinary thermodynamics. Hermann [11] defined the implication of thermodynamic phase space as a differential manifold with a natural contact structure, in which there exists a special subspace of thermodynamic equilibrium states. Weinhold introduced another geometric method in 1975 [12], in which a metric is defined in the space of equilibrium states of thermodynamic systems. Weinhold used the notion of conformal mapping from the Riemannian space to thermodynamic space. Weinhold's metric is defined as the Hessian in the mass representation as follows:

$$g_{ij}^W = \partial_i \partial_j M(S, N^r), \quad (1)$$

where  $M$  is the mass,  $S$  is the entropy, and  $N^r$  is for the other extensive variables of the system. After that, in 1979, Ruppeiner [13] defined a new metric which is the minus signed Hessian in the entropy representation and is given by

$$g_{ij}^R = -\partial_i \partial_j S(M, N^r). \quad (2)$$

The Ruppeiner metric is conformally related to Weinhold's metric as follows [14,15]:

$$ds_R^2 = \frac{1}{T} ds_W^2, \quad (3)$$

where  $T$  is the temperature of the thermodynamic system.

<sup>a</sup>e-mail: [rsk@guilan.ac.ir](mailto:rsk@guilan.ac.ir)

Geometrothermodynamics (GTD) is the latest attempt in this way [16, 17]. Quevedo [16] introduced a general form of the Legendre invariant metric. The general form of the metric in GTD method is as follows:

$$g = \left( E^c \frac{\partial \Phi}{\partial E^c} \right) \left( \eta_{ab} \delta^{bc} \frac{\partial^2 \Phi}{\partial E^c \partial E^d} dE^a dE^d \right), \tag{4}$$

in which

$$\frac{\partial \Phi}{\partial E^c} = \delta_{cb} I^b, \tag{5}$$

where  $E^a$  and  $I^b$  are the extensive and intensive thermodynamic variables and  $\Phi$  is the thermodynamic potential.

There were some alternative and extended theories for General Relativity from the beginning [18–22]. Some of new versions of these theories are trying to justify some observed anomalies on galactic scales (dark matter) and cosmological scales (dark energy) which leads one to reinforce them, such as scalar-tensor theories, brane world cosmology, Lovelock gravity, and  $f(R)$  gravity. Many different aspects, such as cosmic inflation, cosmic acceleration, dark matter, correction of the solar system abnormalities, and also the geodesic motion of test particles have been studied in  $f(R)$  gravity [22–54].

The main purpose of this paper is to investigate that the thermodynamic geometric methods can be used to explain thermodynamics of black holes in  $f(R)$  gravity, and it is organized as follows. In Sect. 2, we review a static black hole in  $f(R)$  gravity, then we study the thermodynamic behavior and thermodynamic geometry methods for this black hole. In Sect. 3, also we review a static charged black hole in  $f(R)$  gravity and study the thermodynamic behavior and thermodynamic geometry methods for it. In Sect. 4, we review a rotating charged black hole in  $f(R)$  gravity, then we investigate the thermodynamic behavior and thermodynamic geometry methods for it, as well, and with the final results we conclude in Sect. 5.

## 2 Static black hole in $f(R)$ gravity

In this section, we study the field equations for a static black hole in  $f(R)$  gravity. The action depending on the Ricci scalar in a generic form is

$$S = \frac{1}{2k} \int d^4x \sqrt{-g} f(R) + S_m. \tag{6}$$

Varying the action with respect to the metric results in the field equations:

$$F(R)R_{\mu\nu} - \frac{1}{2}f(R)g_{\mu\nu} - (\nabla_\mu \nabla_\nu - g_{\mu\nu} \square)F(R) = kT_{\mu\nu}, \tag{7}$$

where  $F(R) = \frac{df(R)}{dr}$  and  $\square = \nabla_\alpha \nabla^\alpha$ .

The generic form of the metric of the spherically symmetric spacetime we are considering is

$$ds^2 = -B(r)dt^2 + A(r)dr^2 + r^2(d\theta^2 + \sin^2\theta d\varphi^2), \tag{8}$$

where  $A(r) = B(r)^{-1}$ . The model employed for  $f(R)$  gravity is given by

$$f(R) = R + \Lambda + \frac{R + \Lambda}{R/R_0 + 2/\alpha} \ln \frac{R + \Lambda}{R_c}, \tag{9}$$

in which  $R_c$  is a constant of integration and  $R_0 = 6\alpha^2/d^2$ , where  $\alpha$  and  $d$ , are free parameters of the action, and also  $\Lambda$  is the cosmological constant. The metric solution up to the first order in the free parameters of the action is obtained:  $B(r) = 1 - \frac{2m}{r} + \beta r - \frac{1}{3}\Lambda r^2$ , where  $\beta = \alpha/d \geq 0$  is a real constant [51, 53].

### 2.1 Thermodynamic

In this section, we study the thermodynamic properties of this black hole. We could find the mass of the black hole  $M$  in terms of its entropy  $S$ , and the radius of curvature of the de Sitter space  $l$ , where  $l$  is related to the cosmological constant  $\Lambda$ , through the relation [55]

$$\Lambda = \frac{3}{l^2}. \tag{10}$$

Using the relation between the entropy  $S$  and the radius of the event horizon  $r_+$ , ( $S = \pi r_+^2$ ), we can write the mass

$$M(S, l, \beta) = \frac{l^2 \pi^{\frac{1}{2}} \beta S + l^2 \pi S^{\frac{1}{2}} - S^{\frac{3}{2}}}{2l^2 \pi^{\frac{3}{2}}}. \tag{11}$$

The other thermodynamic parameters can be calculated by using the above expression as the temperature ( $T = \frac{\partial M}{\partial S}$ ) and the heat capacity ( $C = T \frac{\partial S}{\partial T}$ ) as a function of  $S$ ,  $l$ , and  $\beta$ ,

$$T = \frac{2\beta l^2 \pi^{\frac{1}{2}} S^{\frac{1}{2}} - 3S + l^2 \pi}{4l^2 \pi^{\frac{3}{2}} S^{\frac{1}{2}}}, \tag{12}$$

$$C = -\frac{4\beta l^2 \pi^{\frac{1}{2}} S^{\frac{3}{2}} - 6S^2 + 2l^2 \pi S}{l^2 \pi + 3S}. \tag{13}$$

We have obtained three thermodynamic parameters of this black hole and plotted all of them in terms of the radius of the horizon  $r_+$  (see Figs. 1, 2, and 3).

In Fig. 1, it can be seen that the mass of the black hole becomes zero at two points,  $r_+ = r_{01}$  and  $r_+ = r_{02}$  (we show the zero points of mass with  $r_{01}$  and  $r_{02}$ ), in which  $r_{01} = 0$  and  $r_{02} = 4.0$ , and it reaches a maximum value at  $r_+ = r_m$  (we show the place of the maximum value of the mass by  $r_m$ ), which is equal to 2.31. Also, it can be observed from Fig. 2 that the temperature is positive only in a particular range of  $r_+$ , then it reaches zero at  $r_+ = r_m$  and, after that, it falls into

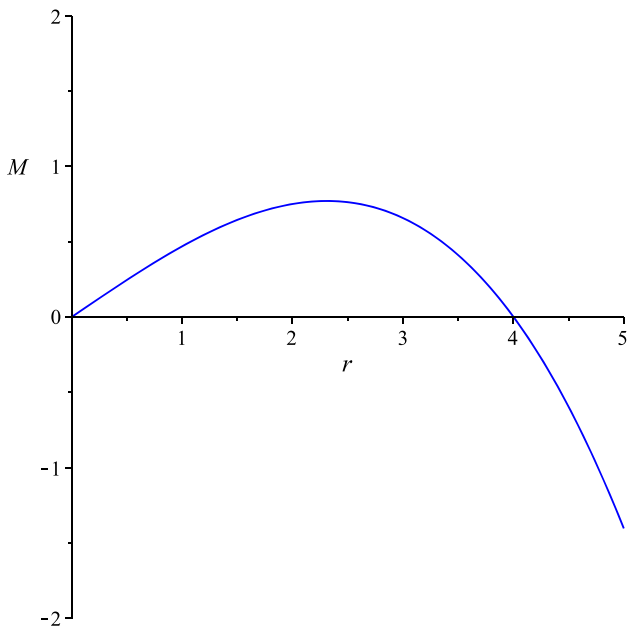


**Fig. 1** Mass variation of a static black hole in terms of the radius of the horizon  $r_+$  for  $l = 4.0, \beta = 10^{-4}$

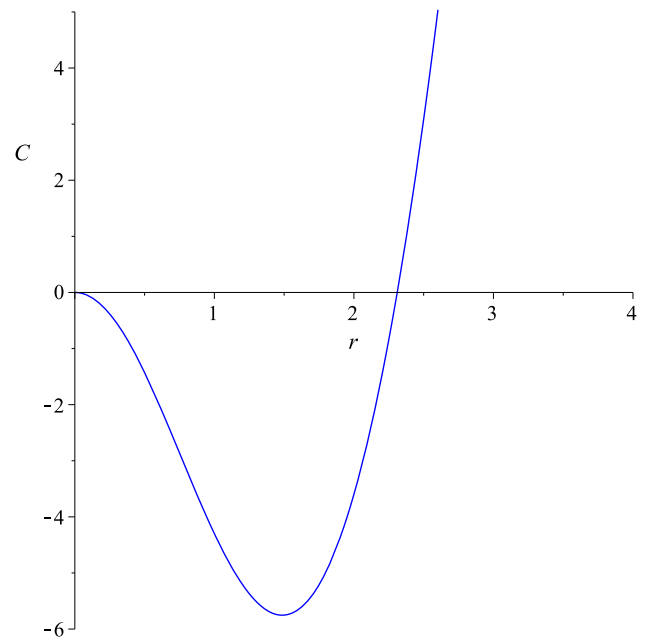


**Fig. 3** Heat capacity variation of a static black hole in terms of the radius of the horizon  $r_+$  for  $l = 4.0, \beta = 10^{-4}$

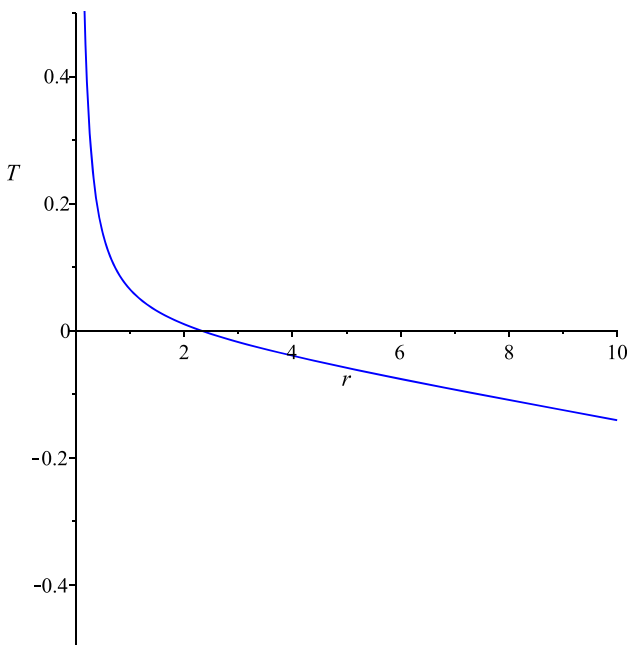


**Fig. 2** Temperature variation of a static black hole in terms of the radius of the horizon  $r_+$  for  $l = 4.0, \beta = 10^{-4}$

the negative region, in which it has no physical meaning. Finally, by plotting the heat capacity of the black hole in terms of the radius of the horizon,  $r_+$ , in Fig. 3, we have shown that this black hole has a phase transition of type one, in other words, in the range of  $0 < r_+ < r_m$ , the heat capacity is in the negative region (unstable phase), then at  $r_+ = r_m$ ,

we have a phase transition of type one ( $C(r_+ = r_m) = 0$ ), after that for,  $r_+ > r_m$ , it will be positive (stable).

### 2.2 Thermodynamic geometry

Now, we construct the geometric structure for this black hole by applying the geometric technique of Weinhold, Ruppeiner, and GTD metrics of the system. In this case, the extensive variables are  $N^r = (l, \beta)$ . According to Eq. (1), we can write the Weinhold metric for this system as

$$g_{ij}^W = \partial_i \partial_j M(S, l, \beta), \tag{14}$$

$$ds_W^2 = M_{SS}dS^2 + M_{ll}dl^2 + M_{\beta\beta}d\beta^2 + 2M_{Sl}dSdl + 2M_{S\beta}dSd\beta + 2M_{l\beta}dl d\beta, \tag{15}$$

therefore

$$g^W = \begin{bmatrix} M_{SS} & M_{Sl} & M_{S\beta} \\ M_{lS} & M_{l\alpha} & 0 \\ M_{\beta S} & 0 & 0 \end{bmatrix}. \tag{16}$$

The components of the above matrix can be found using the expression of  $M$ , given in Eq. (11). We could calculate the curvature scalar of the Weinhold metric as

$$R^W = 0, \tag{17}$$

so the Weinhold structure is flat for this black hole and we cannot explain the phase transition of this thermodynamic system. Now, we use the Ruppeiner method, which is conformally transformed to the Weinhold metric. The Ruppeiner metric is given by

$$ds_R^2 = \frac{1}{T} ds_W^2. \tag{18}$$

The corresponding matrix with the metric components of the Ruppeiner method is as follows:

$$g^R = \left(\frac{1}{T}\right) \begin{bmatrix} M_{SS} & M_{Sl} & M_{S\beta} \\ M_{lS} & M_{ll} & 0 \\ M_{\beta S} & 0 & 0 \end{bmatrix}, \tag{19}$$

which is equal to

$$g^R = \left(\frac{4l^2\pi^{\frac{3}{2}}S^{\frac{1}{2}}}{2l^2\pi^{\frac{1}{2}}S^{\frac{1}{2}}\beta - 3S + l^2\pi}\right) \begin{bmatrix} M_{SS} & M_{Sl} & M_{S\beta} \\ M_{lS} & M_{ll} & 0 \\ M_{\beta S} & 0 & 0 \end{bmatrix}. \tag{20}$$

The curvature of the Ruppeiner metric is obtained:

$$R^R = \frac{4S^{\frac{5}{2}}l^2\pi^{\frac{1}{2}}\beta - 13S^{\frac{5}{2}}\pi^{\frac{1}{2}}l^2\beta - 3S^{\frac{5}{2}}\pi^{\frac{1}{2}}l^2\beta - 11S^2l^2\pi + 3S^3}{4S^3(2S^{\frac{1}{2}}\pi^{\frac{1}{2}}l^2\beta - 3S + l^2\pi)}, \tag{21}$$

which is singular at  $S = 0$  and  $S = \frac{1}{3}l^2\pi(2\beta l(\frac{1}{3}l\beta + \frac{1}{3}\sqrt{l^2\beta^2 + 3}) + 1)$ ; for each solution of  $S$ , there exists a pair of  $r_+$ , ( $r_+ = \pm\sqrt{\frac{S}{\pi}}$ ), which can explain the zero points in this thermodynamic system. We avoid the negative values of this solution because it gives imaginary and negative roots. The values of these zero points are  $r_+ = 0$  and  $r_+ = r_m$ . It is completely coincident with the zero point of the temperature and the heat capacity (the phase transition point) of this black hole. The curvature scalar of the Ruppeiner metric for this black hole with respect to the radius of the horizon,  $r_+$ , is demonstrated in Fig. 4.

Plot of scalar curvature of Ruppeiner metric and heat capacity, in terms of  $r_+$  are shown in Fig. 5. It can be seen from Fig. 5 that singular points of scalar curvature are coincident with the zero point of the heat capacity. Finally, we construct the most important metric in the GTD method, in which a Legendre invariant potential is being used. The metric for this thermodynamic system, according to Eq. (4), is as follows:

$$g^{GTD} = (SM_S + lM_l + \beta M_\beta) \begin{bmatrix} -M_{SS} & 0 & 0 \\ 0 & M_{ll} & 0 \\ 0 & 0 & 0 \end{bmatrix}. \tag{22}$$

We cannot obtain the corresponding curvature scalar with this metric, because the metric determinant is zero, so the inverse of the metric is infinite. Legendre invariance guarantees that the geometric properties of the metric do not depend on the thermodynamic potential used in its construction. Thus, we consider the entropy as the thermodynamical potential [56], and we obtain a new metric using the entropy representation:

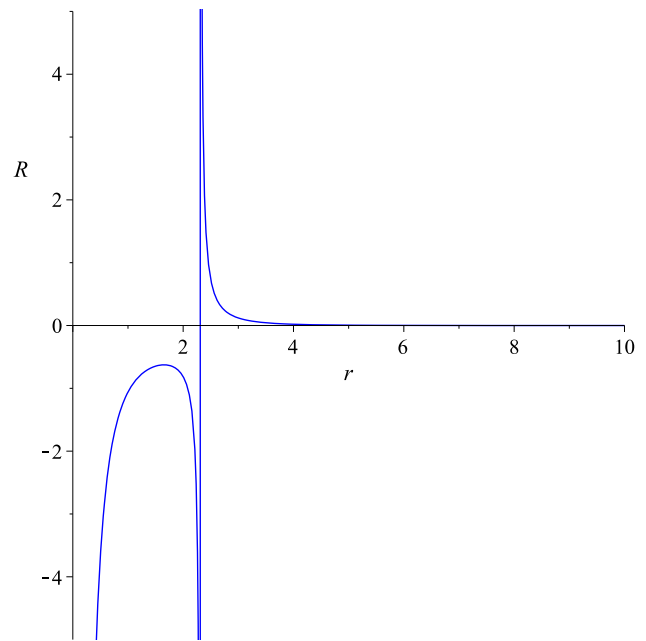


Fig. 4 Variation of the Ruppeiner metric in terms of the radius of the horizon  $r_+$  for  $l = 4.0$ ,  $\beta = 10^{-4}$

$$g^{GTD} = (MS_M + lS_l + \beta S_\beta) \begin{bmatrix} -S_{MM} & 0 & 0 \\ 0 & S_{ll} & S_{l\beta} \\ 0 & S_{\beta l} & S_{\beta\beta} \end{bmatrix}. \tag{23}$$

We use the condition  $M^2l^4 \gg l^6$  to obtain the curvature scalar of this metric, also  $\beta \geq 0.45$  will satisfy this condition. Since the corresponding curvature scalar equation is too large, we demonstrate it in Fig. 6.

It can be seen from Fig. 6 that the curvature scalar of GTD is singular at  $r_+ = 9.21$ . If we plot the heat capacity with this value of  $\beta$ , we see that it will be zero at  $r_+ = 5.37$  (see Fig. 7).

As can be observed from Figs. 6 and 7, the singular point of the curvature scalar is not coincident with a zero point of the heat capacity, so, in this case we cannot find any physical information as regards the system from the GTD method.

Now, at the end of this section, we investigate the effect of changes in the value of  $\beta$  and  $l$ , the parameters on the phase transition points. It is clear from Fig. 8, by a decreasing value of  $\beta$ , that we do not have any changing in the numbers of phase transitions, but the place will decrease. In Fig. 9a, we find that, for small values of  $l$ , the system has phase transition of type one, but for a large value of  $l$ , the system is in the unstable phase and it has no phase transition (see Fig. 9b).

In the next section, we investigate the static charged black hole in  $f(R)$  gravity.

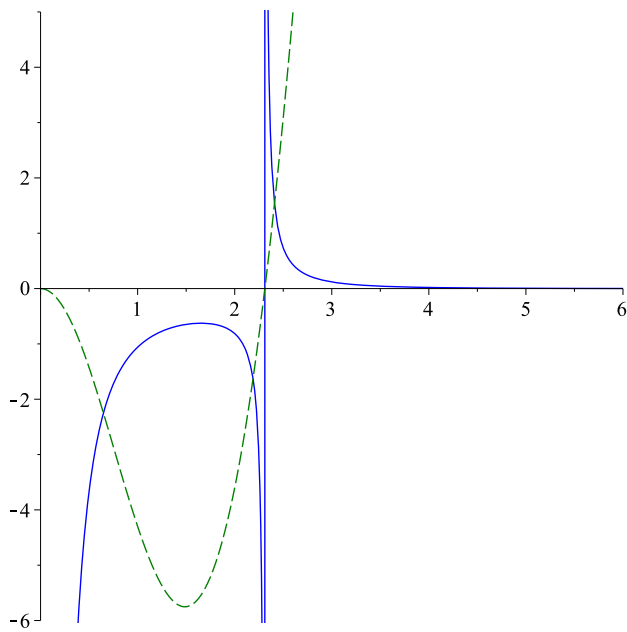


**Fig. 5** Curvature scalar variation of Ruppeiner metric (blue continuous line) and the heat capacity of a static black hole (green dash line) in terms of the radius of the horizon  $r_+$ , for  $l = 4.0$ ,  $\beta = 10^{-4}$

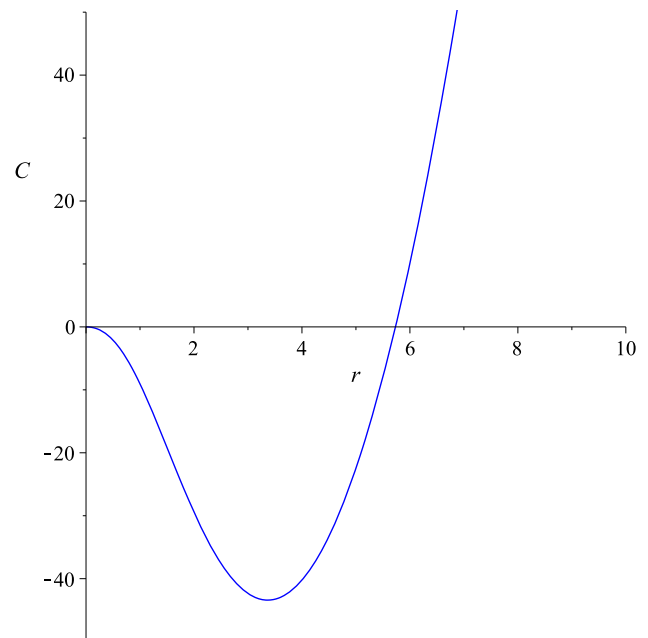


**Fig. 7** Heat capacity variation of a static black hole in terms of the radius of the horizon  $r_+$ , for  $l = 4.0$  and  $\beta = 0.45$

### 3 Static charged black hole in $f(R)$ gravity

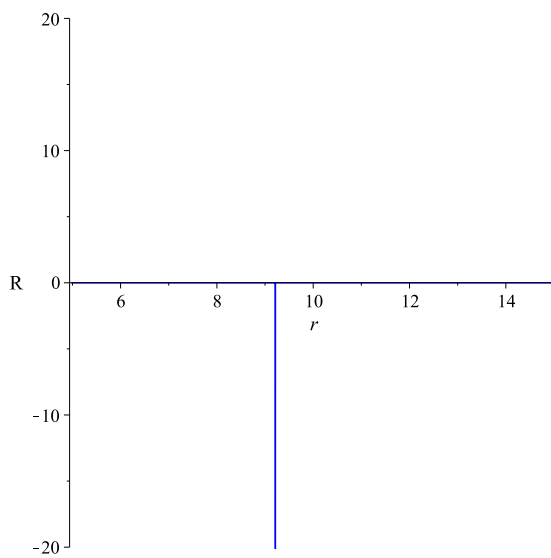
In this section, we describe the metric and the field equations of a static charged black hole in  $f(R)$  gravity. Here, the action for  $f(R)$  gravity, with a Maxwell term in four dimensions, is

$$S = \frac{1}{16\pi G} \int d^4x \sqrt{-g} (R + f(R) - F_{\mu\nu} F^{\mu\nu}). \quad (24)$$

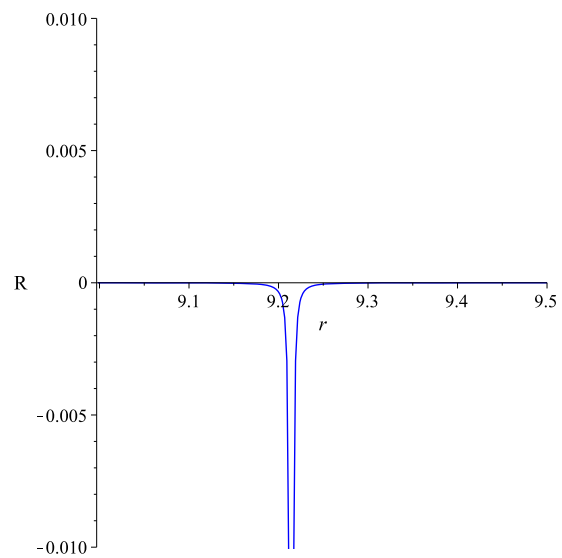
We vary the action with respect to the metric results in the field equations as:

$$R_{\mu\nu}(1 + f'(R)) - \frac{1}{2}(R + f(R))g_{\mu\nu} + (g_{\mu\nu}\nabla^2 - \nabla_\mu\nabla_\nu)f'(R) = 2T_{\mu\nu}, \quad (25)$$

where  $T_{\mu\nu}$  is the stress-energy tensor of the electromagnetic field, which is given by



**(a)**



**(b)** Closeup of figure (a)

**Fig. 6** Variation of curvature scalar of GTD in terms of the radius of the horizon of the black hole  $r_+$ , for  $l = 4.0$  and  $\beta = 0.45$

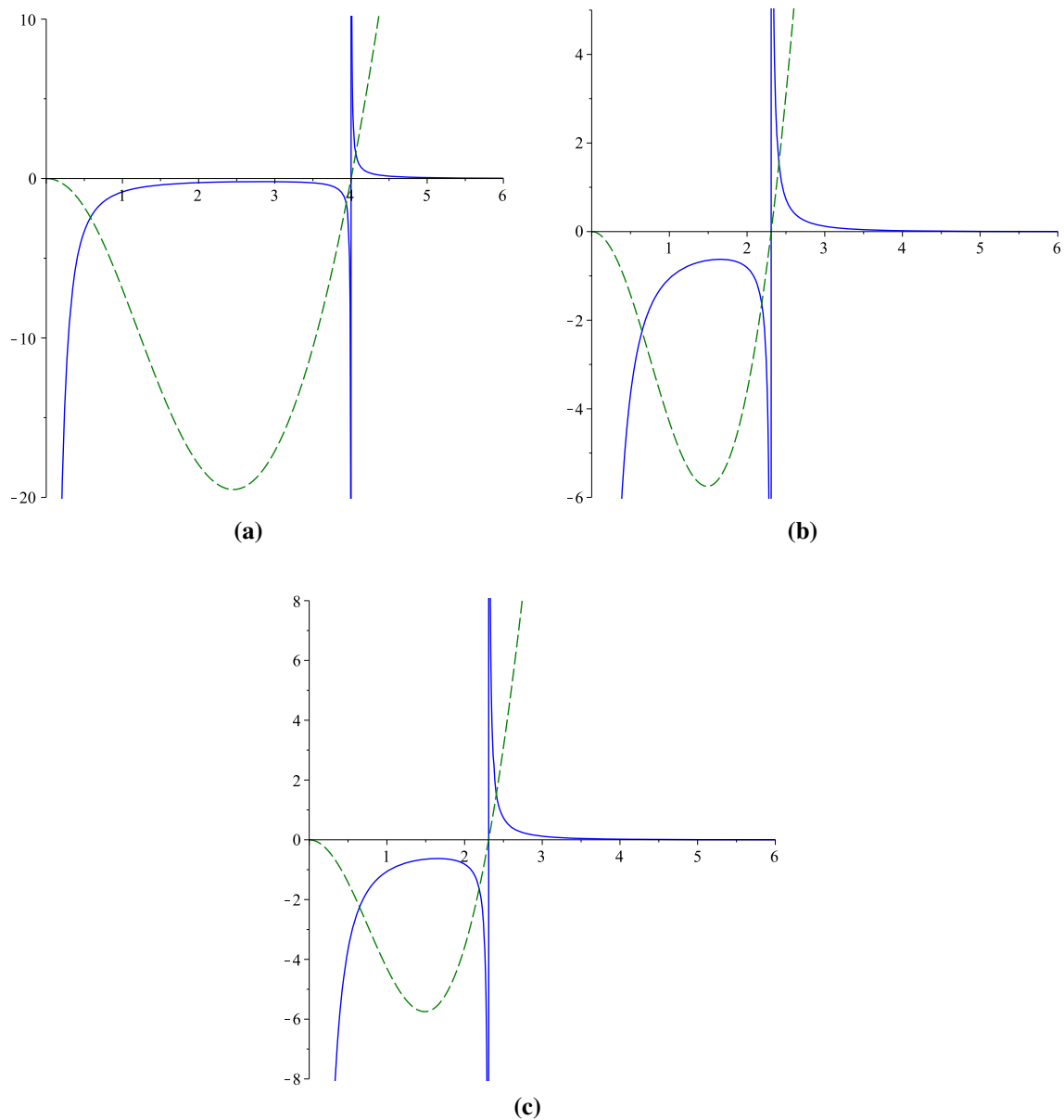


**Fig. 8** Curvature scalar variation of Ruppeiner metric (blue continuous line) and the heat capacity of a static black hole (green dash line) in terms of  $r_+$ , for  $l = 4.0$  and  $\beta = 0.25, \beta = 10^{-4}, \beta = 10^{-15}$ , for **a, b** and **c**, respectively

$$T_{\mu\nu} = F_{\mu\rho} F_{\nu}^{\rho} - \frac{g_{\mu\nu}}{4} F_{\rho\sigma} F^{\rho\sigma}, \tag{26}$$

with

$$T_{\mu}^{\mu} = 0, \tag{27}$$

$R_{\mu\nu}$  is the Ricci tensor, and  $\nabla$  is the usual covariant derivative. The trace of Eq. (25), for  $R = R_0$ , yields

$$R_0(1 + f'(R_0)) - 2(R_0 + f(R_0)) = 0, \tag{28}$$

which determines the negative constant curvature scalar as

$$R_0 = \frac{2f(R_0)}{f'(R_0) - 1}. \tag{29}$$

Using Eqs. (25)–(29), the Ricci tensor is

$$R_{\mu\nu} = \frac{1}{2} \left( \frac{f(R_0)}{f'(R_0) - 1} \right) g_{\mu\nu} + \frac{2}{(1 + f'(R_0))} T_{\mu\nu}. \tag{30}$$

Finally, the metric of the spherically symmetric spacetime is given by

$$ds^2 = N(r)dt^2 - N(r)^{-1}dr^2 - r^2(d\theta^2 + \sin^2\theta d\varphi^2), \tag{31}$$

with

$$N(r) = 1 - \frac{2GM}{r} + \frac{Q^2}{(1 + f'(R_0))r^2} - \frac{1}{12}R_0r^2. \tag{32}$$

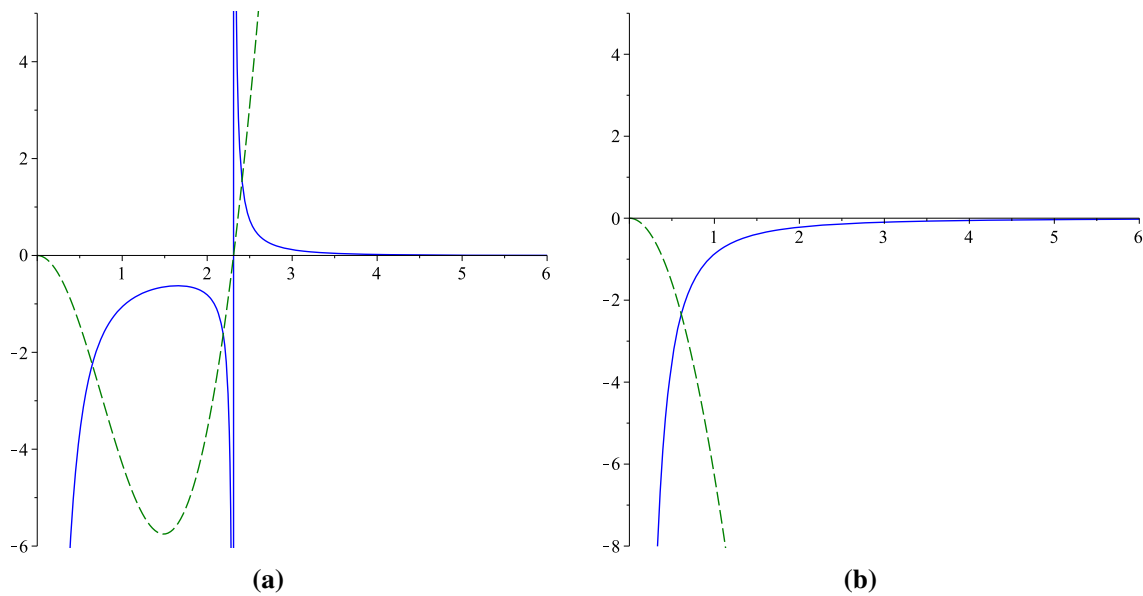


**Fig. 9** Curvature scalar variation of Ruppeiner metric (blue continuous line) and the heat capacity of a static black hole (green dash line) in terms of  $r_+$  for  $\beta = 10^{-4}$ , and  $l = 4.0$ ,  $l = \sqrt{3} \times 10^{15}$ , for **a** and **b**, respectively

For a general discussion of this metric, see Ref. [57]. In the following, we consider  $G = 1$ , and  $q^2 = \frac{Q^2}{(1+f'(R_0))}$ , therefore we have

$$ds^2 = \left(1 - \frac{2M}{r} + \frac{q^2}{r^2} - \frac{1}{12}R_0r^2\right) dt^2 - \left(1 - \frac{2M}{r} + \frac{q^2}{r^2} - \frac{1}{12}R_0r^2\right)^{-1} dr^2 - r^2(d\theta^2 + \sin^2\theta d\varphi^2), \tag{33}$$

where  $R_0 = 4\Lambda$ , in which  $\Lambda$  is the cosmological constant and  $q$  is the electrical charge.

### 3.1 Thermodynamic

In this section we investigate the thermodynamic properties of this black hole. By solving Eq. (32) in terms of  $r_+$  ( $N(r_+) = 0$ ) and, using the relation between the entropy  $S$  and the radius of the horizon  $r_+$ , the mass of this black hole will be obtained in terms of the entropy, charge, and the radius of the de Sitter space, as below:

$$M(S, l, q) = \frac{l^2\pi^2q^2 + l^2\pi S - S^2}{2l^2\pi^{\frac{3}{2}}S^{\frac{1}{2}}}. \tag{34}$$

In the following, we can straightforwardly write the temperature, the electrical potential, and the heat capacity of the black hole, from the first law of thermodynamic as follows:

$$dM = TdS + \Phi dq, \tag{35}$$

$$T = \frac{l^2\pi S - l^2\pi^2q^2 - 3S^2}{4l^2\pi^{\frac{3}{2}}S^{\frac{3}{2}}}, \tag{36}$$

$$\Phi = q\sqrt{\frac{\pi}{S}}, \tag{37}$$

$$C = \frac{2l^2\pi^2q^2S - 2l^2\pi S^2 + 6S^3}{-3l^2\pi^2q^2 + l^2\pi S + 3S^2}. \tag{38}$$

The plots of Eqs. (34)–(38) are demonstrated in Figs. 10, 11, and 12.

Figure 10, shows that the mass of this black hole has a minimum value at  $r_+ = r_{m1}$  (we show the minimum point of the mass by  $r_{m1}$ ), which has a value equal to 0.252, then it reaches its maximum value at  $r_+ = r_{m2}$  (we show the maximum point of mass by  $r_{m2}$ ), at which its value is equal to 2.296, and it vanishes at  $r = r_0$ ,  $r_0$  is the point where the mass becomes zero, and it is equal to 4.0. It is also observed from Fig. 11 that the temperature is positive only in a particular range of event horizon ( $r_{m1} < r_+ < r_{m2}$ ), in addition, at  $r_+ < r_{m1}$ , and  $r_{m2} < r_+$ , it will be negative and it has no physical solution. It can be observed from Fig. 12 that the heat capacity of this black hole will be zero at  $r_{m1}$  and  $r_{m2}$  ( $C(r_+ = r_{m1}) = 0$  and  $C(r_+ = r_{m2}) = 0$ ), in other words, it has two phase transitions of type one at these points, moreover, at  $r_+ = r_\infty$  (we show the divergence point of the heat capacity with  $r_\infty$ ), the heat capacity diverges, and the value of this point is equal to 0.426. In other words, at  $r_+ < r_{m1}$ , the heat capacity is negative and it is in an unstable phase, then, at  $r_{m1} < r_+ < r_\infty$ , the heat capacity is positive or it is in stable phase, afterward, at  $r_\infty < r_+ < r_{m2}$ , it falls

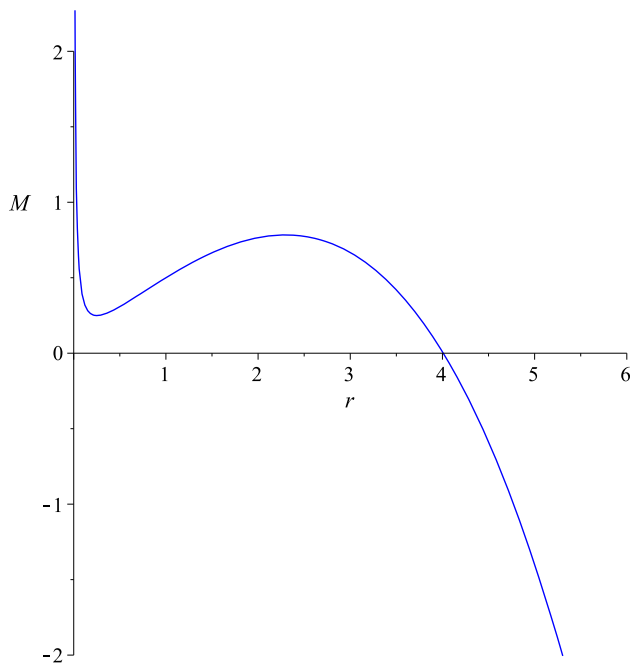


**Fig. 10** Mass variation of a charged static black hole in terms of the radius of the horizon  $r_+$  for  $q = 0.25, l = 4.0$

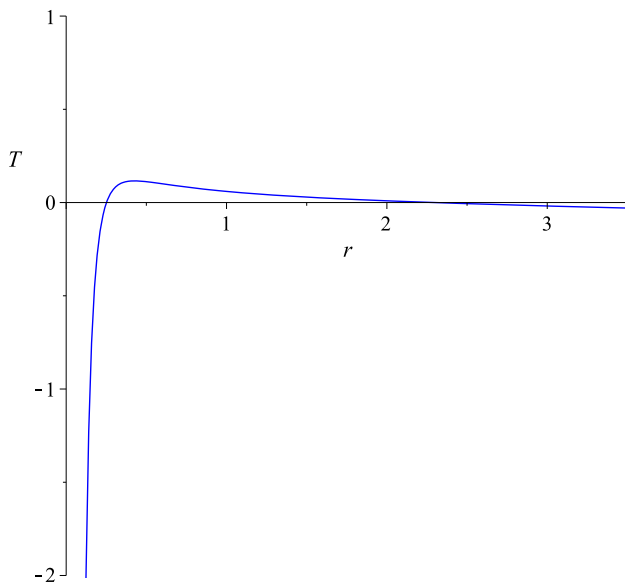


**Fig. 11** Temperature variation of a charged static black hole in terms of the radius of the horizon  $r_+$  for  $q = 0.25, l = 4.0$

in to negative region (unstable phase) and at  $r_+ > r_{m2}$  it becomes stable.

### 3.2 Thermodynamic geometry

In this section, we construct the thermodynamic geometry structure for this black hole. First, we use the Weinhold method. Extensive variables for this system are  $N^r = (l, q)$ , so the resulting matrix of the Weinhold metric becomes

$$g^W = \begin{bmatrix} M_{SS} & M_{Sq} & M_{Sl} \\ M_{qS} & M_{qq} & 0 \\ M_{lS} & 0 & M_{ll} \end{bmatrix}. \tag{39}$$

The elements of the metric can be obtained from Eq. (34), and the Weinhold scalar curvature can be found to be

$$R^W = \frac{9l^2\pi^{\frac{3}{2}}S^{\frac{5}{2}} - l^4\pi^{\frac{7}{2}}q^2S^{\frac{1}{2}} - l^4\pi^{\frac{5}{2}}S^{\frac{3}{2}}}{(l^2\pi^2q^2 - l^2\pi S + 3S^2)^2}. \tag{40}$$

The denominator of the above expression becomes zero at  $S = \frac{\pi l}{6}(l \pm \sqrt{l^2 - 12q^2})$ , or at  $r_+ = r_{m1}$  and  $r_+ = r_{m2}$  (see Fig. 13).

Next, we use the Ruppeiner method for this black hole. Using Eq. (34), the matrix components of Ruppeiner metric will be obtained:

$$g^R = \frac{1}{T} \begin{bmatrix} M_{SS} & M_{Sq} & M_{Sl} \\ M_{qS} & M_{qq} & 0 \\ M_{lS} & 0 & M_{ll} \end{bmatrix}. \tag{41}$$

So, using Eqs. (36) and (41), we obtain

$$g^R = \frac{4l^2\pi^{\frac{3}{2}}S^{\frac{3}{2}}}{l^2\pi S - l^2\pi^2q^2 - 3S^2} \begin{bmatrix} M_{SS} & M_{Sq} & M_{Sl} \\ M_{qS} & M_{qq} & 0 \\ M_{lS} & 0 & M_{ll} \end{bmatrix}. \tag{42}$$

After some calculation, the corresponding curvature scalar will be obtained as

$$R^R = -\frac{l^2\pi(2\pi q^2 - S)}{S(l^2\pi^2q^2 - l^2\pi S + 3S^2)}. \tag{43}$$

This curvature scalar is singular at  $S = 0$  and  $S = \frac{\pi l}{6}(l \pm \sqrt{l^2 - 12q^2})$  or, as can be seen from Fig. 14, it is singular at  $r_+ = 0, r_+ = r_{m1}$ , and  $r_+ = r_{m2}$ .

Finally, we use the most important GTD metric. The matrix resulting from the metric is as follows:

$$g^{GTD} = (SM_S + qM_q + lM_l) \begin{bmatrix} -M_{SS} & 0 & 0 \\ 0 & M_{qq} & 0 \\ 0 & 0 & M_{ll} \end{bmatrix}. \tag{44}$$

The corresponding curvature scalar will be obtained as

$$R^{GTD} = \frac{16}{3} \frac{\mathcal{N}}{(3l^2\pi^2q^2 - l^2\pi S - 3S^2)^2(3l^2\pi^2q^2 + l^2\pi S + S^2)^3}. \tag{45}$$

Here, because the numerator of the above expression has no physical information and it is too long, we consider it as  $\mathcal{N}$ . The denominator of  $R^{GTD}$  becomes zero at  $r_+ = r_{\infty}$  (see Fig. 15). So, we extended our study to different thermodynamical geometries. It can be observed from Fig. 16 that the Weinhold and Ruppeiner methods are compatible with zeros of the heat capacity, and GTD method is coincident with the divergences of it. In the following, we point out the effect of different values of the spacetime parameters on the stability conditions of this black hole. As can be seen from Fig. 17a,



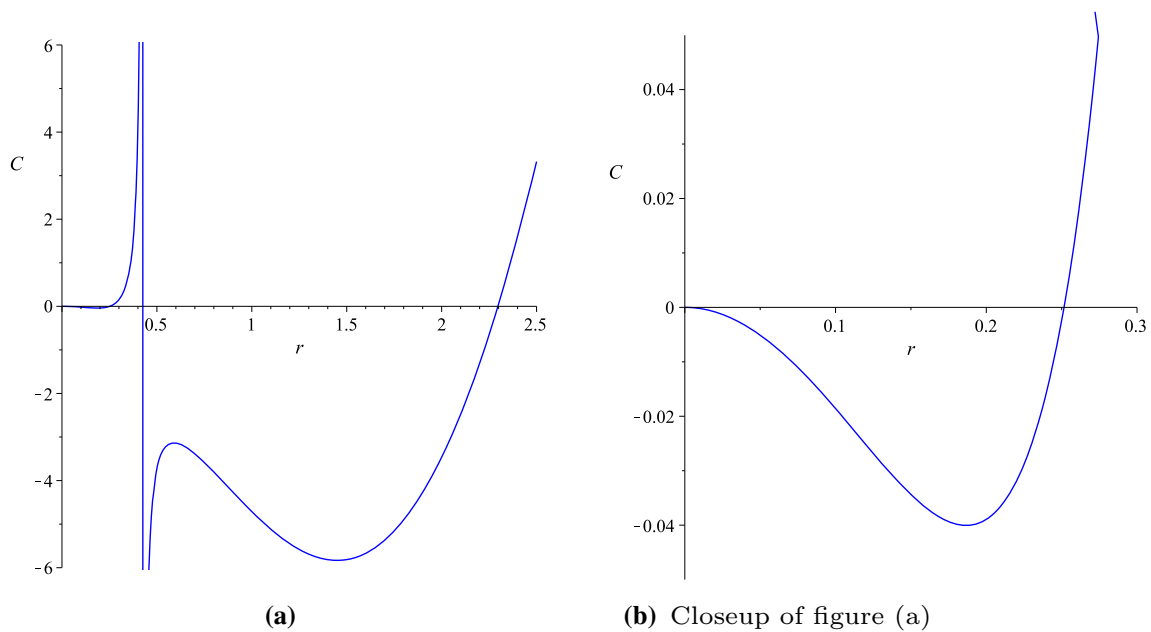


**Fig. 12** Heat capacity variation of a charged static black hole in terms of the radius of the horizon,  $r_+$  for  $l = 4.0, q = 0.25$

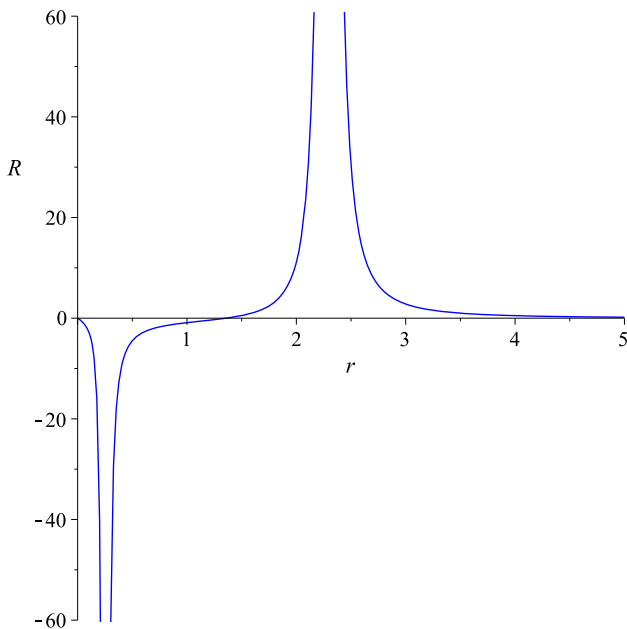


**Fig. 13** Curvature scalar variation of the Weinhold metric in terms of the radius of the horizon  $r_+$  for  $l = 4.0, q = 0.25$

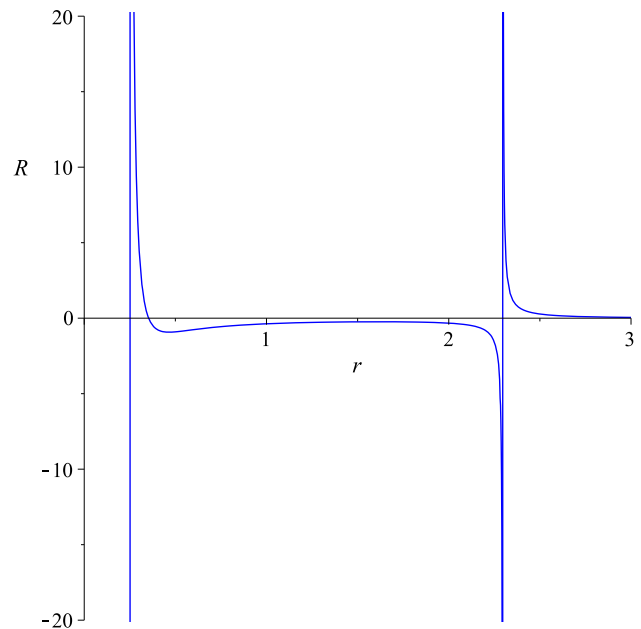


**Fig. 14** Curvature scalar variation of the Ruppeiner metric in terms of the radius of the horizon  $r_+$  for  $l = 4.0, q = 0.25$

for  $q = 0$ , the heat capacity of this black hole can be treated like the black hole in the previous section and it has only one phase transition, of type one. By increasing the value of  $q$ , it will have two phase transitions of type one and one phase transition of type two. Also, for small values of  $l$ , the heat capacity has two phase transitions of type one and one phase transition of type two (see Fig. 18a, b), and for large values of  $l$ , it has one phase transition of type one and one phase transition of type two (see Fig. 18c, d).

In the next section, we study the thermodynamic behavior of a rotating charged black hole in  $f(R)$  gravity.

#### 4 Rotating charged black hole in $f(R)$ gravity

In this section, we study the solution of the field equation and metric of a rotating charged black hole in  $f(R)$  gravity. With a Maxwell term in four dimensions, the action is

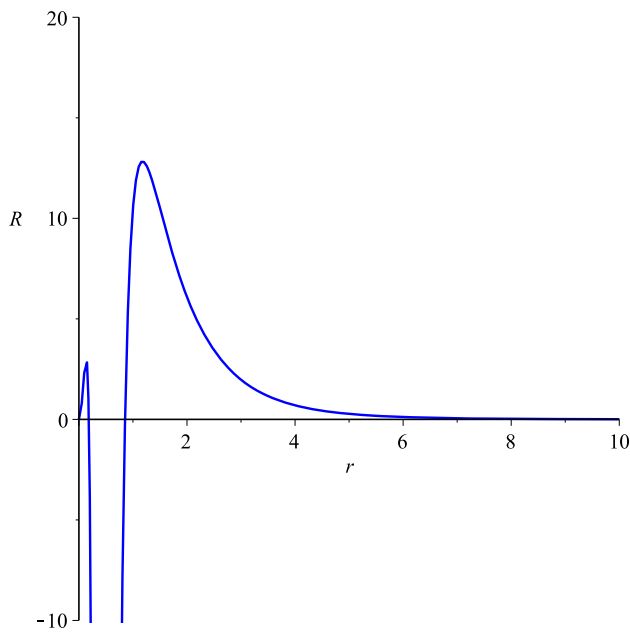


**Fig. 15** Curvature scalar variation of GTD metric in terms of the radius of the horizon  $r_+$  for  $l = 4.0, q = 0.25$

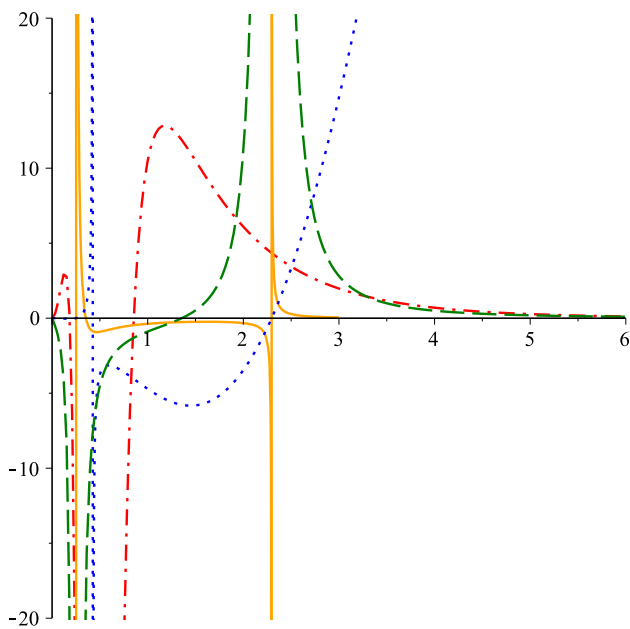


**Fig. 16** Curvature scalar variation of GTD (red dash-dot line), the Ruppeiner (orange continuous line) and the Weinhold (green dash line) metrics, and the heat capacity (blue dot line), in terms of the radius of the horizon  $r_+$ , for  $l = 4.0, q = 0.25$

$$S = S_g + S_M, \tag{46}$$

where  $S_g$  is the gravitational action,

$$S_g = \frac{1}{16\pi} \int d^D x \sqrt{|g|} (R + f(R)), \tag{47}$$

and  $S_M$  is the electromagnetic action,

$$S_M = \frac{-1}{16\pi} \int d^4 x \sqrt{-g} [F_{\mu\nu} F^{\mu\nu}], \tag{48}$$

where  $R$  is the scalar curvature and  $R + f(R)$  is the function defining the theory under consideration, and  $g$  is the determinant of the metric. From Eq. (48), the Maxwell equation takes the form

$$\nabla_\mu F^{\mu\nu} = 0. \tag{49}$$

The field equations in the metric formalism are [58]

$$R_{\mu\nu} (1 + f'(R)) - \frac{1}{2} (R + f(R)) g_{\mu\nu} + (g_{\mu\nu} \nabla^2 - \nabla_\mu \nabla_\nu) f'(R) = 2T_{\mu\nu}, \tag{50}$$

where  $\nabla$  is the usual covariant derivative,  $R_{\mu\nu}$  is the Ricci tensor, and  $T_{\mu\nu}$  the stress-energy tensor of the electromagnetic field,

$$T_{\mu\nu} = F_{\mu\rho} F_\nu^\rho - \frac{g_{\mu\nu}}{4} F_{\rho\sigma} F^{\rho\sigma}, \tag{51}$$

with

$$T^\mu_\mu = 0. \tag{52}$$

The trace of Eq. (50) with the constant curvature scalar  $R = R_0$  yields

$$R_0 (1 + f'(R_0)) - 2(R_0 + f(R_0)) = 0, \tag{53}$$

which determines the negative constant curvature scalar as

$$R_0 = \frac{2f(R_0)}{f'(R_0) - 1}. \tag{54}$$

Using Eqs. (50)–(54), we have

$$R_{\mu\nu} = \frac{1}{2} \left( \frac{f(R_0)}{f'(R_0) - 1} \right) g_{\mu\nu} + \frac{2}{(1 + f'(R_0))} T_{\mu\nu}. \tag{55}$$

Finally, the axisymmetric ansatz in Boyer–Lindquist-type coordinates  $(t, r, \theta, \varphi)$ , inspired by the Kerr–Newman–AdS black hole solution, is [58]

$$ds^2 = -\frac{\Delta_r}{\rho^2} \left[ dt - \frac{a \sin^2 \theta d\varphi}{\mathcal{E}} \right]^2 + \frac{\rho^2}{\Delta_r} dr^2 + \frac{\rho^2}{\Delta_\theta} d\theta^2 + \frac{\Delta_\theta \sin^2 \theta}{\rho^2} \left[ a dt - \frac{r^2 + a^2}{\mathcal{E}} d\varphi \right]^2, \tag{56}$$

where

$$\Delta_r = (r^2 + a^2) \left( 1 + \frac{R_0}{12} r^2 \right) - 2mr + \frac{Q^2}{(1 + f'(R_0))}, \tag{57}$$

$$\begin{aligned} \mathcal{E} &= 1 - \frac{R_0}{12} a^2, & \rho^2 &= r^2 + a^2 \cos^2 \theta, \\ \Delta_\theta &= 1 - \frac{R_0}{12} a^2 \cos^2 \theta, \end{aligned} \tag{58}$$

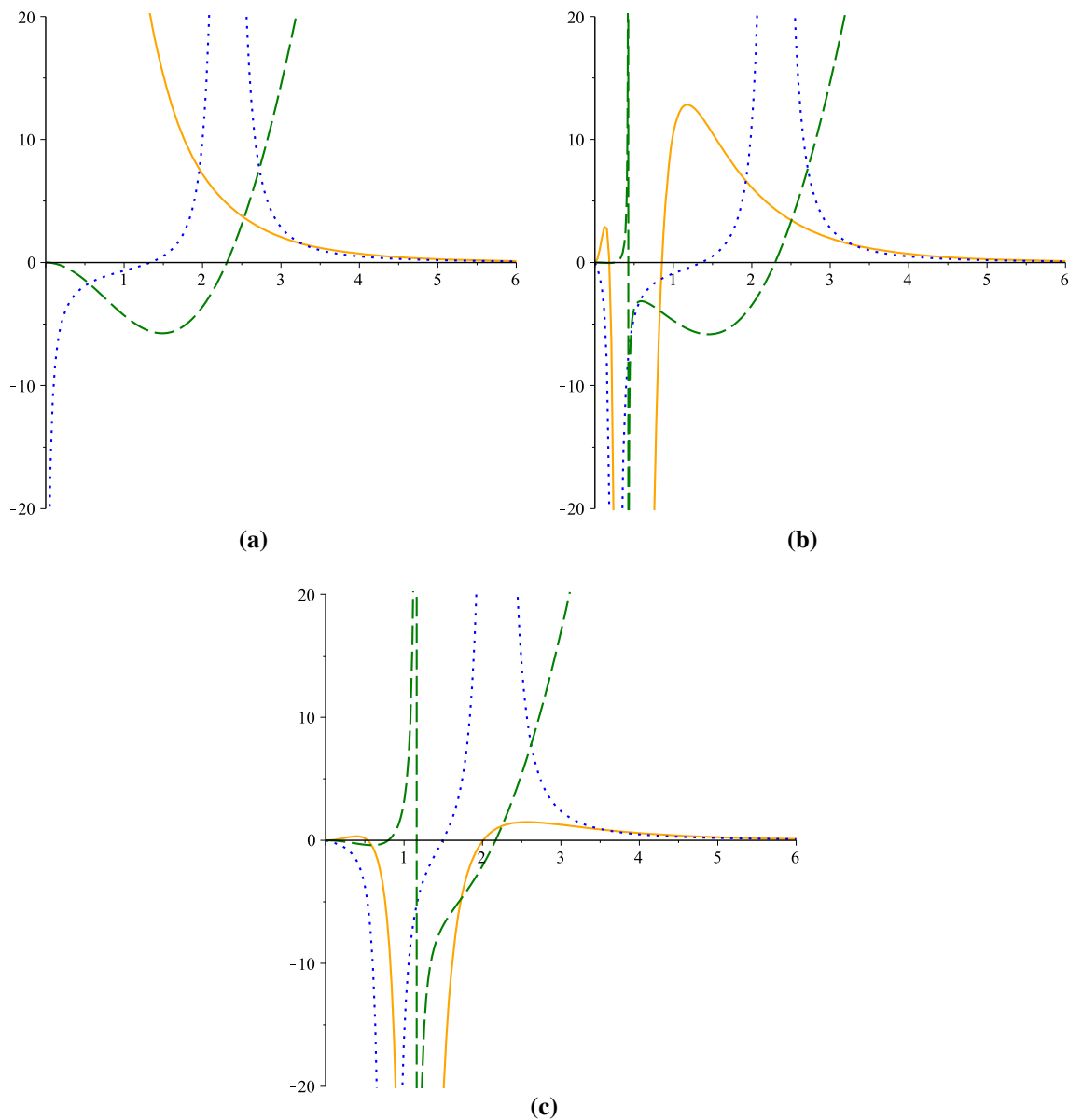


**Fig. 17** Curvature scalar variation of GTD (orange continuous line), the Weinhold (blue dot line) metrics, and the heat capacity (green dash line) in terms of  $r_+$ , for  $l = 4.0$  and  $q = 0, q = 0.25, q = 0.75$ , for **a, b, and c**, respectively

in which  $R_0$ , is a constant proper to cosmological constant ( $R_0 = -4\Lambda$ ),  $Q$  is the electric charge, and  $a$  is the angular momentum per mass of the black hole.

#### 4.1 Thermodynamic

In this section, we investigate the thermodynamic properties of this black hole. The radius of the horizon ( $r_+$ ) satisfies the condition, with  $\Delta_r = 0$ ,

$$(r_+^2 + a^2) \left( 1 + \frac{R_0}{12} r_+^2 \right) - 2mr_+ + \frac{Q^2}{(1 + f'(R_0))} = 0. \tag{59}$$

By setting  $dr = dt = 0$  in the metric line elements, we can find the line elements for the 2-dimensional horizon. Using the relation

$$A = \int_0^{2\pi} d\varphi \int_0^\pi \sqrt{|\gamma|} d\theta, \tag{60}$$

where  $\gamma$  is the metric tensor of the black hole horizon, the area of this black hole will be obtained as

$$A = \frac{4\pi(r_+^2 + a^2)}{1 - \frac{R_0}{12} a^2}. \tag{61}$$

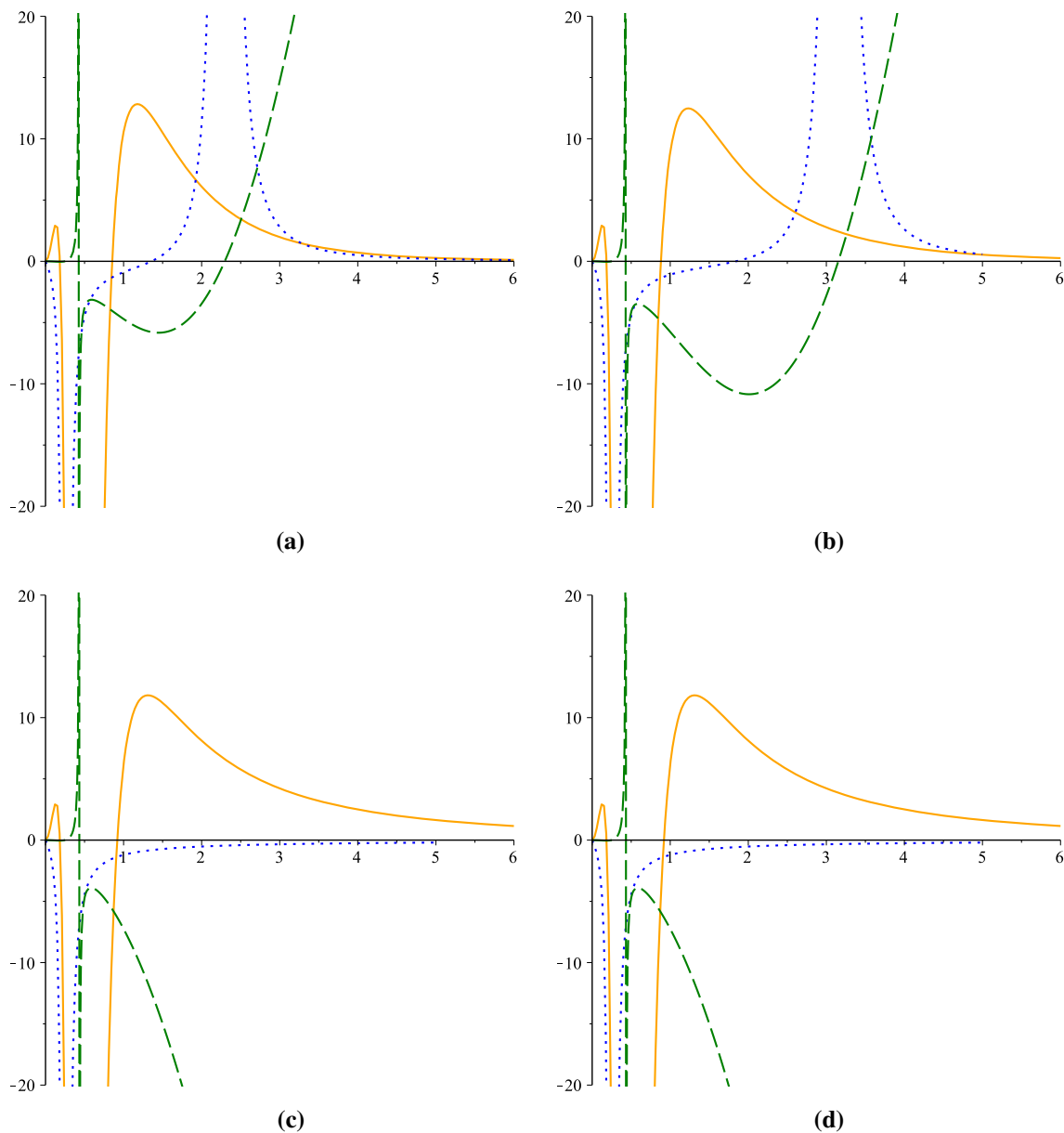


**Fig. 18** Curvature scalar variation of GTD (orange continuous line), the Weinhold (blue dot line) metrics, and the heat capacity (green dash line) in terms of  $r_+$ , for  $q = 0.25$  and  $l = 4.0, l = \sqrt{30}, l = \sqrt{3} \times 10^4, l = \sqrt{3} \times 10^{15}$ , for **a, b, c, and d**, respectively

According to the relation for the entropy  $S = \frac{A}{4}$  [2], we can easily find the entropy of this black hole,

$$S = \frac{\pi(r_+^2 + a^2)}{1 - \frac{R_0}{12}a^2}. \tag{62}$$

The mass of the black hole can be obtained by using a generalized Smarr formula in terms of all its parameters. To calculate the generalized Smarr formula, first we obtain the total mass ( $M$ ), and the angular momentum ( $J$ ), by means of Komar integrals and using the Killing vectors,  $\frac{1}{\Xi}\partial_t$ , and  $\partial_\varphi$ , so they will be obtained thus

$$M = \frac{m}{\Xi^2}, \tag{63}$$

$$J = \frac{am}{\Xi^2}. \tag{64}$$

Using Eqs. (59)–(64), the generalized Smarr formula will be obtained:

$$M^2 = \frac{S}{4\pi} + \frac{\pi}{4S}[4J^2 + q^4] + \frac{q^2}{2} - \frac{R_0}{12}J^2 - \frac{R_0S}{24\pi} \left[ q^2 + \frac{S}{\pi} - \frac{R_0S^2}{24\pi^2} \right]. \tag{65}$$

Now, according to the first law of thermodynamic, we can calculate all of the thermodynamic quantities,

$$dM = TdS + \Omega dJ + \Phi dq. \tag{66}$$

So, the temperature of this black hole is

$$T = \frac{\partial M}{\partial S} = -(48q^4\pi^5 + 8R_0\pi^3R_0S^2q^2 + 192\pi^5J^2 - R_0^2\pi S^4 + 16R_0\pi^2S^3 - 48\pi^3S^2) \times (256\pi^4S^3(144\pi^5q^4 - 48R_0\pi^4J^2S - 24R_0\pi^3q^2S^2 + 576\pi^5J^2 + 288\pi^4q^2S + R_0^2\pi S^4 - 24R_0\pi^2S^3 + 144\pi^3S^2))^{-\frac{1}{2}}. \tag{67}$$

In addition, the angular velocity  $\Omega$  is

$$\Omega = \frac{\partial M}{\partial J} = -(2\pi^2J(R_0S - 12\pi)) \times (S(144\pi^5q^4 - 48R_0\pi^4J^2S - 24R_0\pi^3q^2S^2 + 576\pi^5J^2 + 288\pi^4q^2S + R_0^2\pi S^4 - 24R_0\pi^2S^3 + 144\pi^3S^2))^{-\frac{1}{2}}, \tag{68}$$

and also the electrical potential can be obtained:

$$\Phi = \frac{\partial M}{\partial q} = -\pi q(-12\pi^2q^2 + R_0S^2 - 12\pi S) \times (S(144\pi^5q^4 - 48R_0\pi^4J^2S - 24R_0\pi^3q^2S^2 + 576\pi^5J^2 + 288\pi^4q^2S + R_0^2\pi S^4 - 24R_0\pi^2S^3 + 144\pi^3S^2))^{-\frac{1}{2}}. \tag{69}$$

Finally, we can calculate the heat capacity of this black hole as follows:

$$C = \frac{\partial_S M}{\partial_S^2 M}. \tag{70}$$

Plot of all thermodynamic parameters obtained for this black hole are shown in Figs. 19, 20, and 21.

It can be seen from Fig. 19 that the mass of this black hole has one minimum point at  $r_+ = r_m$  (we show the place of the minimum point of the mass with  $r_m$ ), in which the value is equal to 0.252. It is also observed from the plot of the temperature in Fig. 20 that the temperature of this system is in the negative region at a particular range of  $r_+$  ( $r_+ < r_m$ ); after that, it reaches to zero at  $r_+ = r_m$ , then it will be positive for  $r_+ > r_m$ . In addition, Fig. 21 shows that the heat capacity of this black hole reaches a positive (stable) phase from a negative (unstable) phase, and after that it reaches zero at  $r_+ = r_m$ . Also the divergence points of the heat capacity are  $r_{\infty 1}$  and  $r_{\infty 2}$ , and for this system  $r_{\infty 1} = 0.466$  and  $r_{\infty 2} = 2.266$ . So, for the range of  $r_m < r_+ < r_{\infty 1}$ , the heat capacity is positive and system is in the stable phase; after that, at  $r_{\infty 1} < r_+ < r_{\infty 2}$ , it falls into the negative region (unstable phase), then at  $r_+ > r_{\infty 2}$  it will be positive (stable). In other

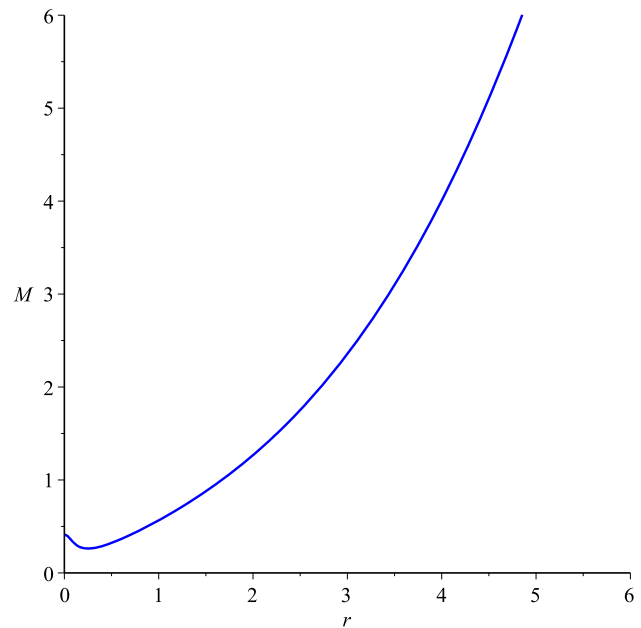


**Fig. 19** Mass variation of a rotating charged black hole in terms of its radius of the horizon  $r_+$  for  $l = 4.0, a = 0.1, q = 0.25$

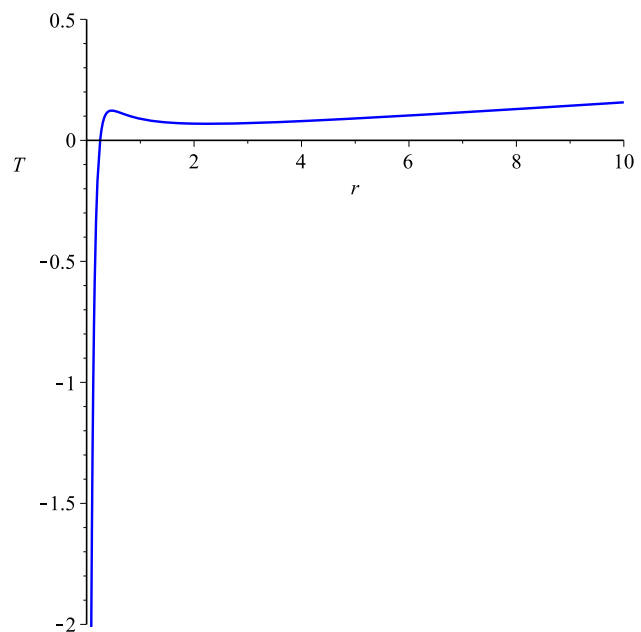


**Fig. 20** Temperature variation of a Rotating charged black hole in terms of its radius of the horizon  $r_+$  for  $l = 4.0, a = 0.1, q = 0.25$

words, the heat capacity of this black hole has one phase transition of type one, and two phase transitions of type two.

#### 4.2 Thermodynamic geometry

In this part, we investigate thermodynamic geometry of this black hole, using the Weinhold, Ruppeiner, and GTD meth-

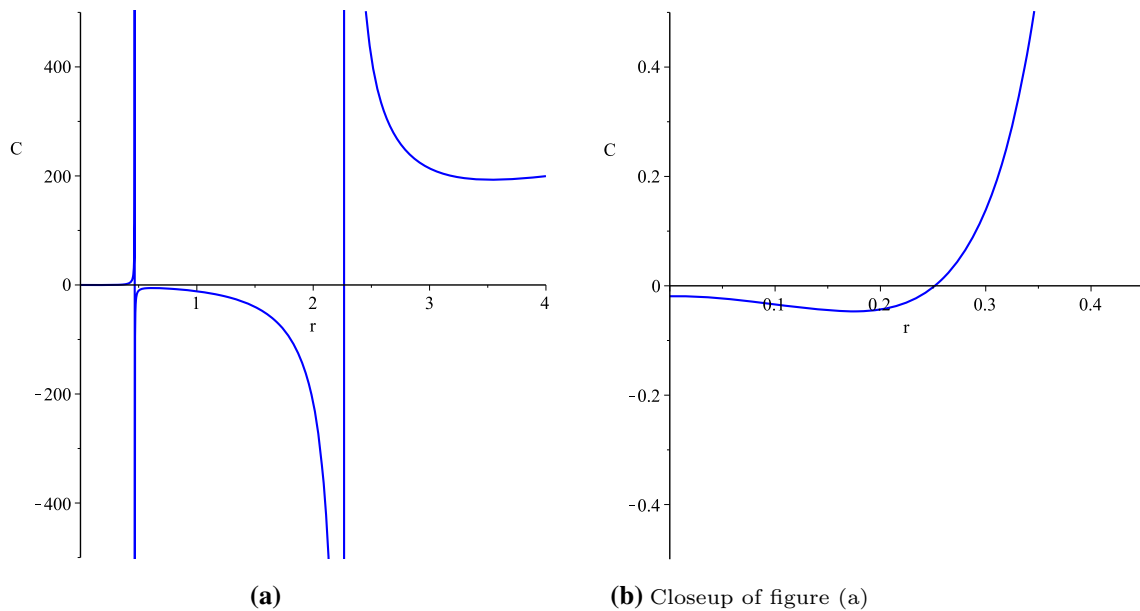


**Fig. 21** Heat capacity variation of a Rotating charged black hole in terms of the radius of the horizon  $r_+$ , for  $l = 4.0, a = 0.1, q = 0.25$

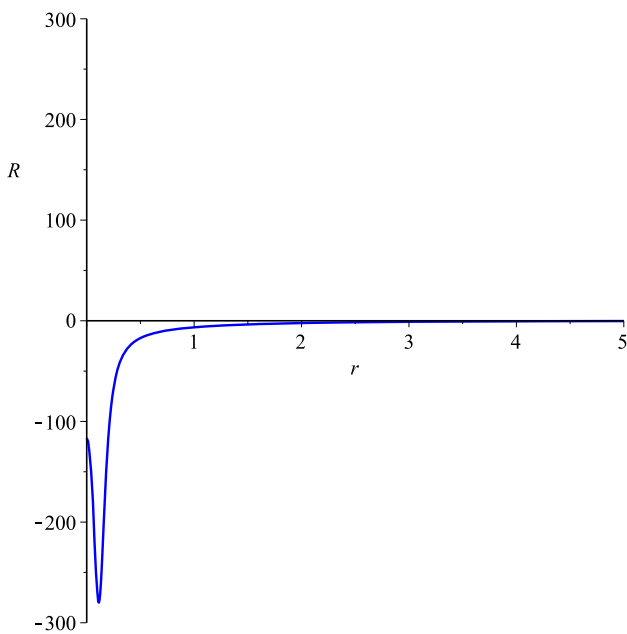


**Fig. 22** Curvature scalar variation of Weinhold metric in terms of the radius of the horizon  $r_+$  for  $l = 4.0, q = 0.25, a = 0.1$

ods. We start by the Weinhold metric, which is as follows:

$$g^W = \begin{bmatrix} M_{SS} & M_{SJ} & M_{Sq} & M_{Sl} \\ M_{JS} & M_{JJ} & M_{Jq} & M_{Jl} \\ M_{qS} & M_{qJ} & M_{qq} & M_{lq} \\ M_{lS} & M_{lJ} & M_{lq} & M_{ll} \end{bmatrix}. \tag{71}$$

The scalar curvature  $R^W$  can easily be obtained; it is plotted in Fig. 22.

It can be seen from Fig. 22 that the curvature scalar has no singularity, so the Weinhold method has no physical information for this system.

Now, we construct the Ruppeiner metric for this black hole as follows:

$$g^R = \frac{1}{T} \begin{bmatrix} M_{SS} & M_{SJ} & M_{Sq} & M_{Sl} \\ M_{JS} & M_{JJ} & M_{Jq} & M_{Jl} \\ M_{qS} & M_{qJ} & M_{qq} & M_{lq} \\ M_{lS} & M_{lJ} & M_{lq} & M_{ll} \end{bmatrix}, \tag{72}$$

where  $T$  can be obtained from Eq. (67). The curvature scalar, which corresponds to the above metric, is plotted in Fig. 23, and it is singular at  $r_+ = r_m$ .

Finally, at the end of this section, we apply the most important metric of the GTD method to this thermodynamic system,

$$g^{GTD} = \begin{bmatrix} -M_{SS} & 0 & 0 & 0 \\ 0 & M_{JJ} & M_{Jq} & M_{Jl} \\ 0 & M_{qJ} & M_{qq} & M_{lq} \\ 0 & M_{lJ} & M_{lq} & M_{ll} \end{bmatrix}. \tag{73}$$

A plot of the corresponding curvature scalar with the GTD metric is shown in Fig. 24.

This curvature scalar is singular at  $r_+ = r_{\infty 1}$  and  $r_+ = r_{\infty 2}$ . So, again we extended our study to different geothermodynamic methods, and our results are shown in Fig. 25. It can be observed from Fig. 25 that a singularity of the Ruppeiner metric is compatible with the zero point of the heat capacity, and singularities of the GTD metric are coincident with the divergence points of the heat capacity. At the end of this section, we investigate the effect of different values of

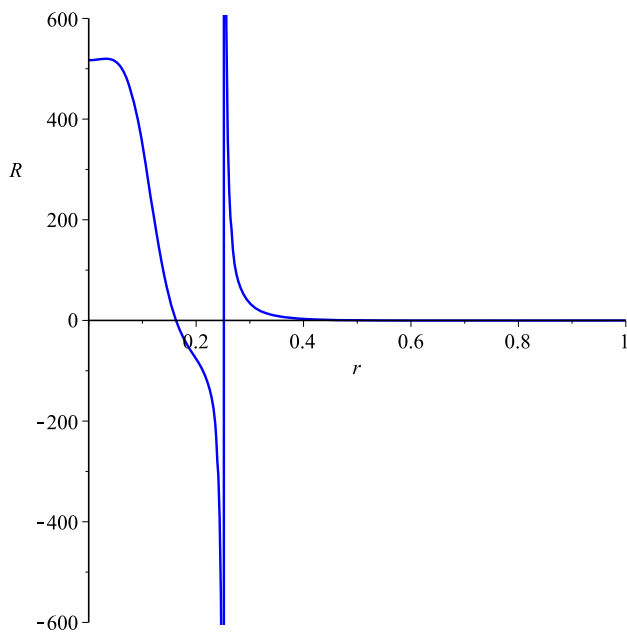


**Fig. 23** Curvature scalar variation of the Ruppeiner metric in terms of the radius of the horizon  $r_+$ .  $l = 4.0$  for  $q = 0.25$ ,  $a = 0.1$

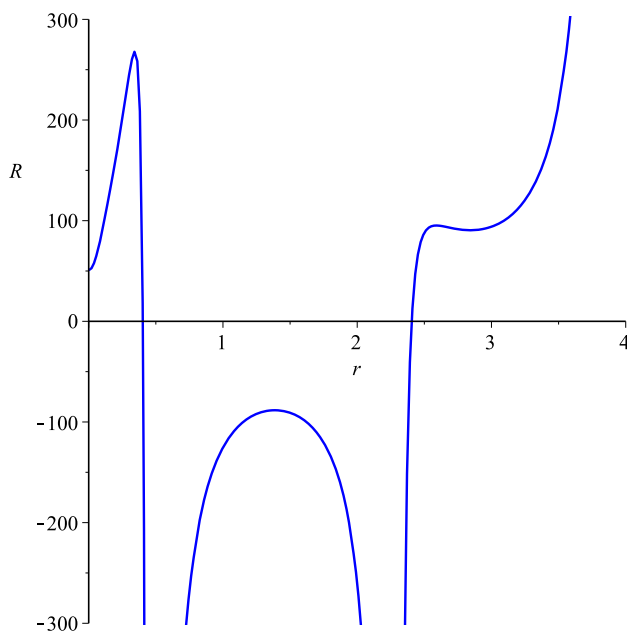


**Fig. 24** Curvature scalar variation of the GTD metric in terms of the radius of the horizon  $r_+$  for  $l = 4.0$ ,  $a = 0.1$ , and  $q = 0.25$

the  $q$ ,  $a$ , and  $l$ , parameters on the phase transition points for this system.

In Figs. 26, 27 and 28, we plot the curvature scalar of the Ruppeiner and GTD metrics with the heat capacity of this black hole. It can be seen from Figs. 26a, 27a, and 28a that this thermodynamical system has one phase transition of type one and two phase transitions of type two. The number of these phase transitions changes for different values of the  $q$ ,  $a$ , and

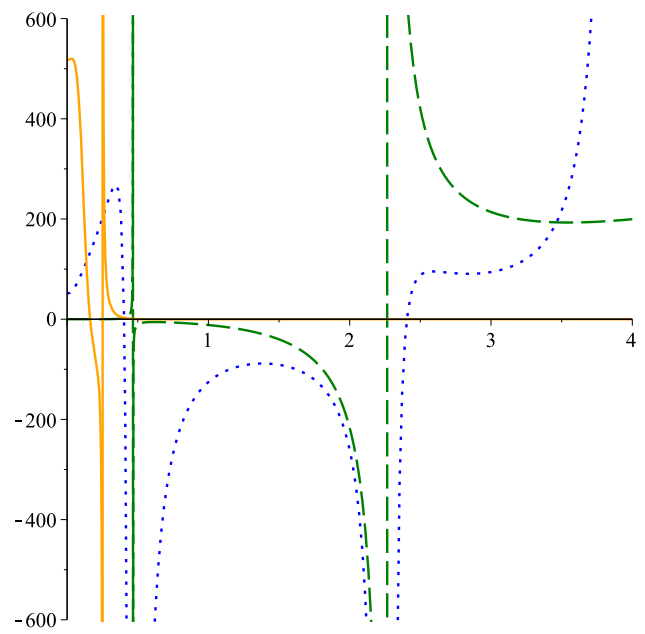


**Fig. 25** Curvature scalar variation of the Ruppeiner (orange continuous line) and GTD (blue dot line) metrics, and the heat capacity (green dash line) of a rotating black hole in terms of  $r_+$  for  $l = 4.0$ ,  $a = 0.1$ ,  $q = 0.25$

$l$ , parameters. By increasing the value of  $q$ , the number of phase transitions will be decreased, as can be observed from Fig. 26c, d; it has only one phase transition of type one. Also, by increasing the value of  $a$ , the number of phase transitions will be decreased, as shown in Fig. 27d, it has two phase transitions of type two. Moreover, by increasing the value of  $l$ , the number of phase transitions will be decreased, and it has only one phase transition of type two (see Fig. 28c, d).

### 5 Conclusion

In this paper, we studied the thermodynamic behavior of three types (static, charged static, and charged rotating) of black holes in  $f(R)$  gravity, and we investigated the thermodynamic geometry of them. Also, we plotted thermodynamic quantities in terms of the radius of the horizon  $r_+$  and we showed that for each maximum and minimum value of the mass, these black holes have one zero point in their temperature and heat capacity. When we applied the thermodynamic geometry methods to these black holes, we have seen that, for a static black hole, the Weinhold metric is flat, and the Ruppeiner metric can explain the zero points of it. For the static charged black hole, the Weinhold and Ruppeiner metrics coincide with the zero points of the heat capacity, and the GTD metric can explain the divergence point of it as well. Moreover, for the rotating charged black hole, the Weinhold metric has no singularity, but the Ruppeiner metric

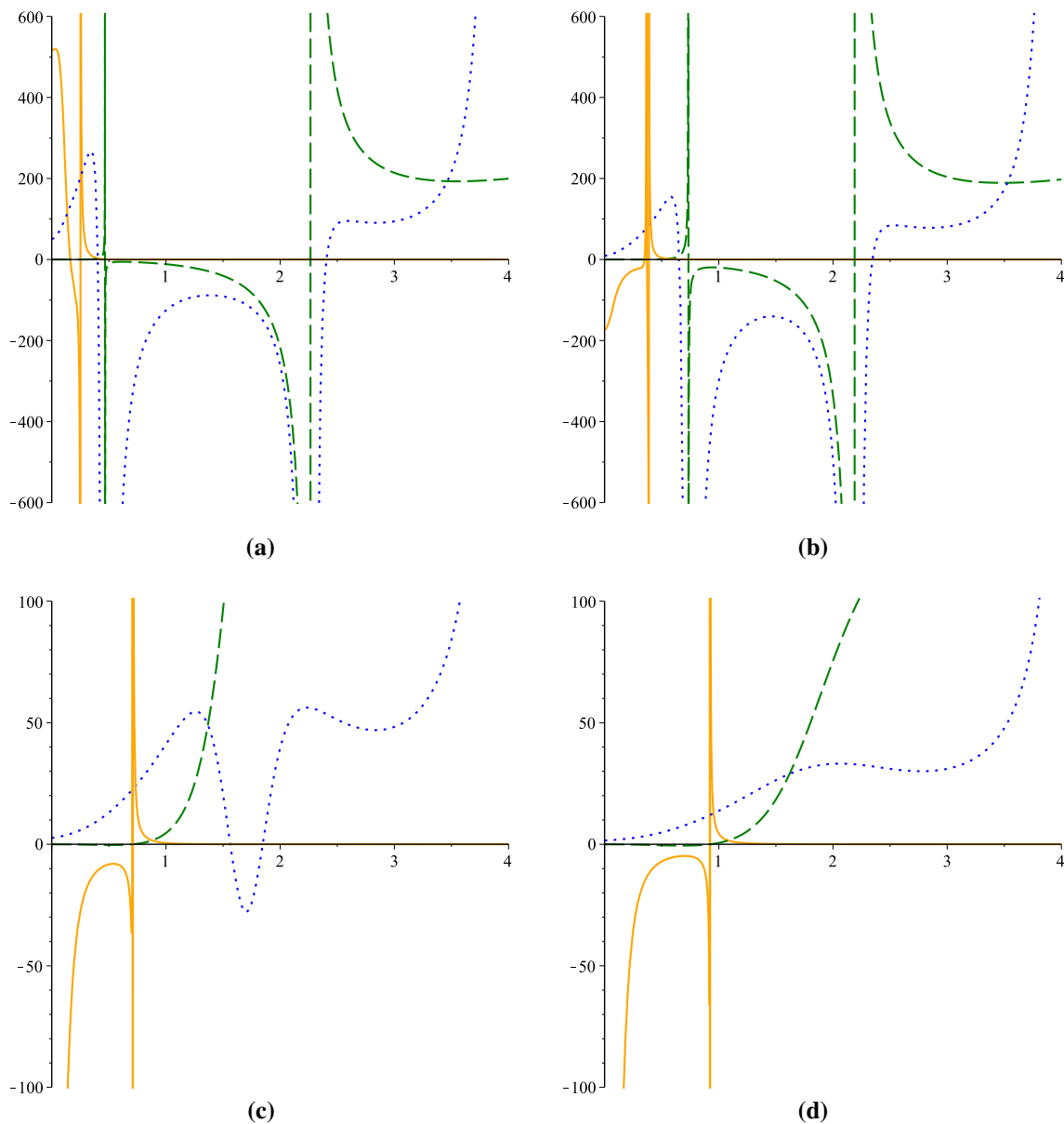


**Fig. 26** Curvature scalar variation of the Ruppeiner (orange continuous line) and GTD (blue dot line) metrics and the heat capacity (green dash line) of a rotating black hole in terms of  $r_+$  for  $l = 4.0$ ,  $a = 0.1$  and  $q = 0.25$ ,  $q = 0.4$ ,  $q = 0.75$ ,  $q = 1$ , for **a**, **b**, **c** and **d**, respectively

can explain the zero points of the heat capacity and the GTD metric coincides with the divergence point of it.

We also investigated the effects of different values of the spacetime parameters on the stability conditions of these black holes. We observed that, by changing the values of the spacetime parameters, the number of phase transitions

of these black holes is changed. But these changes have not affected the compatibility of the explained thermodynamical geometry methods with zeros and divergence points of the heat capacity.

For future work, it would be interesting to apply these methods to other spacetimes such as dilaton black holes.



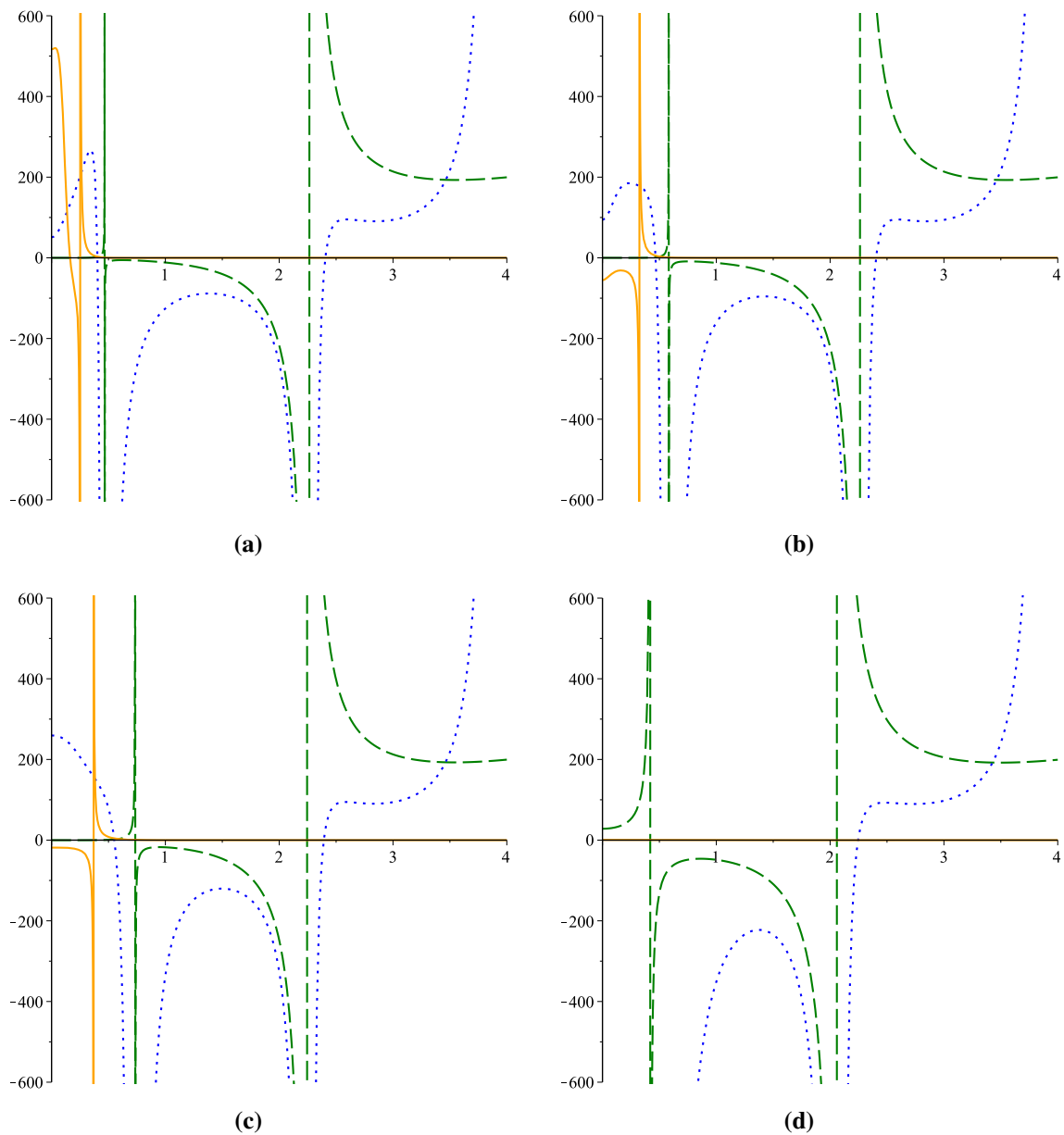


**Fig. 27** Curvature scalar variation of the Ruppeiner (orange continuous line) and GTD (blue dot line) metrics, and the heat capacity (green dash line) of a rotating black hole in terms of  $r_+$  for  $l = 4.0$ ,  $q = 0.25$  and  $a = 0.1$ ,  $a = 0.25$ ,  $a = 0.5$ ,  $a = 0.8$ , for **a**, **b**, **c** and **d**, respectively

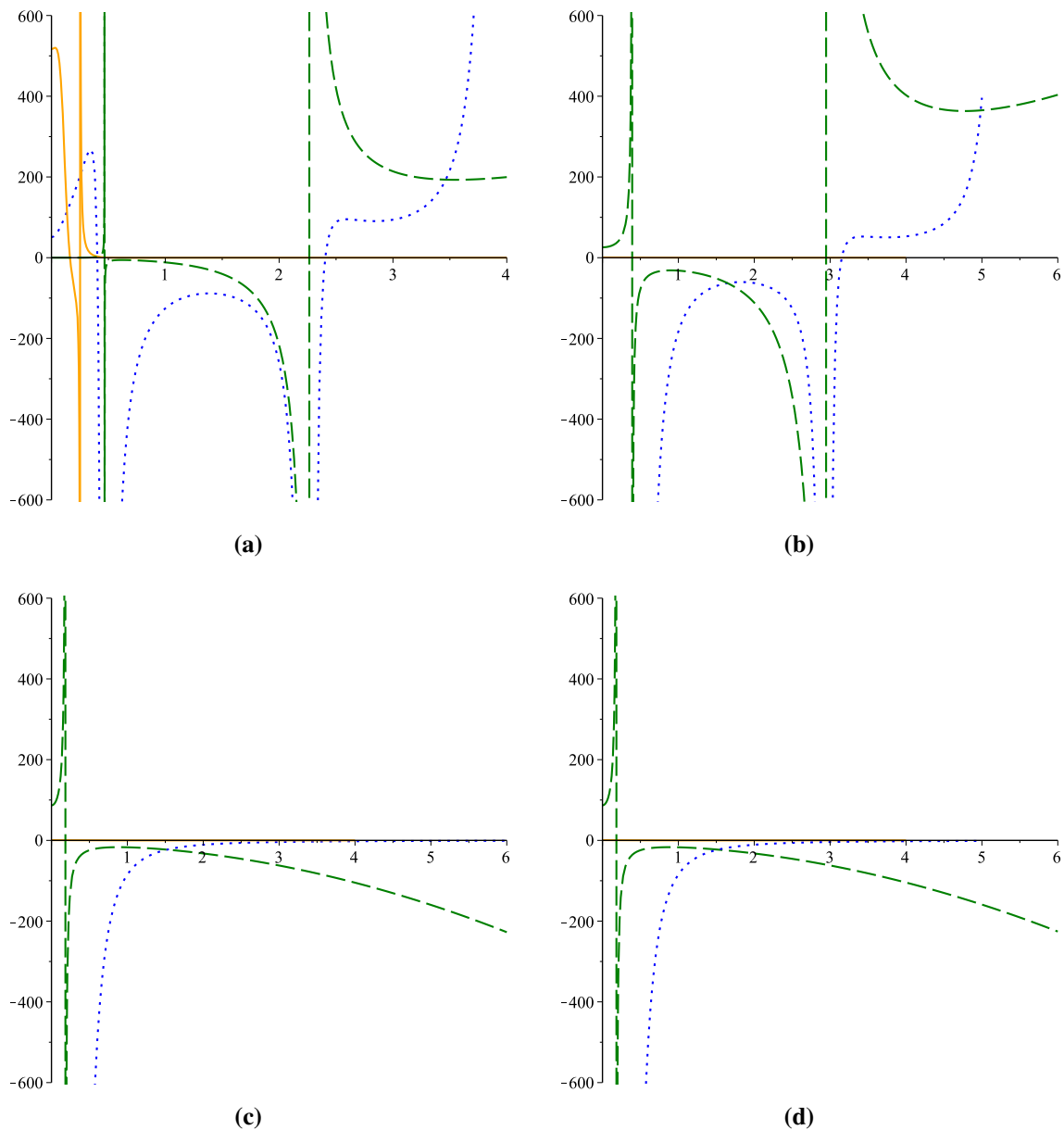


**Fig. 28** Curvature scalar variation of the Ruppeiner (*orange continuous line*) and GTD (*blue dot line*) metrics, and the heat capacity (*green dash line*) of a rotating black hole in terms of  $r_+$  for  $q = 0.25$ ,  $a = 0.1$ , and  $l = 4.0, l = \sqrt{30}, l = \sqrt{3} \cdot 10^4, l = \sqrt{3} \cdot 10^{15}$ , for **a, b, c** and **d**, respectively

**Open Access** This article is distributed under the terms of the Creative Commons Attribution 4.0 International License (<http://creativecommons.org/licenses/by/4.0/>), which permits unrestricted use, distribution, and reproduction in any medium, provided you give appropriate credit to the original author(s) and the source, provide a link to the Creative Commons license, and indicate if changes were made. Funded by SCOAP<sup>3</sup>.

## References

1. S.W. Hawking, *Nature* **248**, 30 (1974)
2. J.D. Bekenstein, *Phys. Rev. D* **7**, 2333 (1973)
3. S.W. Hawking, *Commun. Math. Phys.* **43**, 199 (1975) [Erratum: *Commun. Math. Phys.* **46**, 206 (1976)]
4. D. Kothawala, T. Padmanabhan, S. Sarkar, *Phys. Rev. D* **78**, 104018 (2008). [arXiv:0807.1481](https://arxiv.org/abs/0807.1481) [gr-qc]
5. T. Padmanabhan, *Class. Quantum Gravity* **21**, 4485 (2004). [arXiv:gr-qc/0308070](https://arxiv.org/abs/gr-qc/0308070)
6. J.D. Bekenstein, *Lett. Nuovo Cim.* **4**, 737 (1972)
7. Y.S. Myung, *Phys. Rev. D* **77**, 104007 (2008). [arXiv:0712.3315](https://arxiv.org/abs/0712.3315) [gr-qc]
8. B.M.N. Carter, I.P. Neupane, *Phys. Rev. D* **72**, 043534 (2005). [arXiv:gr-qc/0506103](https://arxiv.org/abs/gr-qc/0506103)
9. D. Kastor, S. Ray, J. Traschen, *Class. Quantum Gravity* **26**, 195011 (2009). [arXiv:0904.2765](https://arxiv.org/abs/0904.2765) [hep-th]
10. F. Capela, G. Nardini, *Phys. Rev. D* **86**, 024030 (2012). [arXiv:1203.4222](https://arxiv.org/abs/1203.4222) [gr-qc]

11. R. Hermann, *Geometry, Physics and Systems* (Marcel Dekker, New York, 1973)
12. F. Weinhold, J. Chem. Phys. **63**, 2479 (1975)
13. G. Ruppeiner, Phys. Rev. A **20**, 1608 (1979)
14. R. Mrugala, Physica A (Amsterdam) **125**, 631 (1984)
15. P. Salamon, J.D. Nulton, E. Ihrig, J. Chem. Phys. **80**, 436 (1984)
16. H. Quevedo, J. Math. Phys. **48** (2007) 013506. [arXiv:physics/0604164](#)
17. H. Quevedo, Gen. Relativ. Gravit. **40**, 971 (2008). [arXiv:0704.3102 \[gr-qc\]](#)
18. H. Weyl, Ann. Phys. **59**, 101 (1919)
19. H. Weyl, Surv. High Energy Phys. **5**, 237 (1986)
20. H. Weyl, Ann. Phys. **364**, 101 (1919)
21. A.S. Eddington, *The Mathematical Theory of Relativity* (Cambridge University Press, Cambridge, 1923)
22. C. Brans, R.H. Dicke, Phys. Rev. **124**, 925 (1961)
23. A.G. Riess et al. (Supernova Search Team Collaboration), Astron. J. **116**, 1009 (1998). [arXiv:astro-ph/9805201](#)
24. S. Perlmutter et al. (Supernova Cosmology Project Collaboration), Astrophys. J. **517**, 565 (1999). [arXiv:astro-ph/9812133](#)
25. J.L. Tonry et al. (Supernova Search Team Collaboration), Astrophys. J. **594**, 1 (2003). [arXiv:astro-ph/0305008](#)
26. C.L. Bennett et al. (WMAP Collaboration), Astrophys. J. Suppl. **148**, 1 (2003). [arXiv:astro-ph/0302207](#)
27. G. Hinshaw et al. (WMAP Collaboration), Astrophys. J. Suppl. **170**, 288 (2007). [arXiv:astro-ph/0603451](#)
28. Y. Fujii, K. Maeda, *The Scalar–Tensor Theory of Gravitation* (Cambridge University Press, Cambridge, 2003)
29. T.P. Sotiriou, Class. Quantum Gravity **23**, 5117 (2006). [arXiv:gr-qc/0604028](#)
30. P. Brax, C. van de Bruck, Class. Quantum Gravity **20**, R201 (2003). [arXiv:hep-th/0303095](#)
31. L.A. Gergely, Phys. Rev. D **74**, 024002 (2006). [arXiv:hep-th/0603244](#)
32. M. Demetrian, Gen. Relativ. Gravit. **38**, 953 (2006). [arXiv:gr-qc/0506028](#)
33. D. Lovelock, J. Math. Phys. **12**, 498 (1971)
34. D. Lovelock, J. Math. Phys. **13**, 874 (1972)
35. S.H. Hendi, M.H. Dehghani, Phys. Lett. B **666**, 116 (2008). [arXiv:0802.1813 \[hep-th\]](#)
36. M.H. Dehghani, R. Pourhasan, Phys. Rev. D **79**, 064015 (2009). [arXiv:0903.4260 \[gr-qc\]](#)
37. S.H. Hendi, S. Panahiyan, H. Mohammadpour, Eur. Phys. J. C **72**, 2184 (2012). [arXiv:1501.05841 \[gr-qc\]](#)
38. A. Sheykhi, H. Moradpour, N. Riazi, Gen. Relativ. Gravit. **45**, 1033 (2013). [arXiv:1109.3631 \[physics.gen-ph\]](#)
39. H.A. Buchdahl, Mon. Not. Roy. Astron. Soc. **150**, 1 (1970)
40. A.A. Starobinsky, Phys. Lett. B **91**, 99 (1980)
41. K. Bamba, S.D. Odintsov, JCAP **0804**, 024 (2008). [arXiv:0801.0954 \[astro-ph\]](#)
42. M. Akbar, R.G. Cai, Phys. Lett. B **648**, 243 (2007). [arXiv:gr-qc/0612089](#)
43. G. Cognola, E. Elizalde, S. Nojiri, S.D. Odintsov, L. Sebastiani, S. Zerbini, Phys. Rev. D **77**, 046009 (2008). [arXiv:0712.4017 \[hep-th\]](#)
44. C. Corda, Int. J. Mod. Phys. D **18**, 2275 (2009). [arXiv:0905.2502 \[gr-qc\]](#)
45. S. Capozziello, F. Darabi, D. Vernieri, Mod. Phys. Lett. A **25**, 3279 (2010). [arXiv:1009.2580 \[gr-qc\]](#)
46. S.H. Hendi, D. Momeni, Eur. Phys. J. C **71**, 1823 (2011). [arXiv:1201.0061 \[gr-qc\]](#)
47. S. Asgari, R. Saffari, Gen. Relativ. Gravit. **44**, 737 (2012). [arXiv:1104.5108 \[gr-qc\]](#)
48. S.H. Mazharimousavi, M. Halilsoy, T. Tahamtan, Eur. Phys. J. C **72**, 1958 (2012). [arXiv:1109.3655 \[gr-qc\]](#)
49. S.G. Ghosh, S.D. Maharaj, U. Papnoi, Eur. Phys. J. C **73**(6), 2473 (2013). [arXiv:1208.3028 \[gr-qc\]](#)
50. S.H. Hendi, B. Eslam Panah, R. Saffari, Int. J. Mod. Phys. D **23**, 1450088 (2014). [arXiv:1408.5570 \[hep-th\]](#)
51. R. Saffari, S. Rahvar, Phys. Rev. D **77**, 104028 (2008). [arXiv:0708.1482 \[astro-ph\]](#)
52. S. Chakraborty, S. SenGupta, Eur. Phys. J. C **75**(1), 11 (2015). [arXiv:1409.4115 \[gr-qc\]](#)
53. S. Soroushfar, R. Saffari, J. Kunz, C. Lämmerzahl, Phys. Rev. D **92**(4), 044010 (2015). [arXiv:1504.07854 \[gr-qc\]](#)
54. S. Chakraborty, S. SenGupta, Eur. Phys. J. C **75**(11), 538 (2015). [arXiv:1504.07519 \[gr-qc\]](#)
55. R. Tharanath, J. Suresh, N. Varghese, V.C. Kuriakose, Gen. Relativ. Gravit. **46**, 1743 (2014). [arXiv:1404.6789 \[gr-qc\]](#)
56. H. Quevedo, A. Sanchez, S. Taj, A. Vazquez, Gen. Relativ. Gravit. **43**, 1153 (2011). doi:10.1007/s10714-010-0996-2. [arXiv:1010.5599 \[gr-qc\]](#)
57. T. Moon, Y.S. Myung, E.J. Son, Gen. Relativ. Gravit. **43**, 3079 (2011). [arXiv:1101.1153 \[gr-qc\]](#)
58. A. Larranaga, Pramana. J. Phys. **78**, 697 (2012). [arXiv:1108.6325 \[gr-qc\]](#)